

A deterministic optimization algorithm for nonconvex and combinatorial bi-objective programming

Ye Seol Lee^{a,b}, George Jackson^a, Amparo Galindo^a, Claire S. Adjiman^{*,a}

^a*Department of Chemical Engineering, Sargent Centre for Process Systems Engineering, Institute for Molecular Science and Engineering, Imperial College London, South Kensington Campus, London SW7 2AZ, United Kingdom*

^b*Department of Chemical Engineering, University College London, Torrington Pl, London WC1E 7JE, United Kingdom*

Abstract

Many practical multiobjective optimization (MOO) problems include discrete decision variables and/or nonlinear model equations and exhibit disconnected or smooth but nonconvex Pareto surfaces. Scalarization methods, such as the weighted-sum and sandwich (SD) algorithms, are common approaches to solving MOO problems but may fail on nonconvex or discontinuous Pareto fronts. In the current work, motivated by the well-known normal boundary intersection (NBI) method and the SD algorithm, we present SDNBI, a new algorithm for bi-objective optimization (BOO) designed to address the theoretical and numerical challenges associated with the reliable solution of general nonconvex and discrete BOO problems. The main improvements in the algorithm are the effective exploration of the nonconvex regions of the Pareto front and, uniquely, the early identification of regions where no additional Pareto solutions exist. The performance of the SDNBI algorithm is assessed based on the accuracy of the approximation of the Pareto front constructed over the disconnected nonconvex objective domains. The new algorithm is compared with two MOO approaches, the modified NBI method and the SD algorithm, using published benchmark problems. The results indicate that the SDNBI algorithm outperforms the modified NBI and SD algorithms in solving convex, nonconvex-continuous, and combinatorial problems, both in terms of computational cost and of the overall quality of the Pareto-optimal set, suggesting that the SDNBI algorithm is a promising alternative for solving BOO problems.

Keywords: sandwich algorithm, normal boundary intersection, nonconvex and discrete multiobjective optimization

1. Introduction

Many real-world problems in operational research, engineering, biology, and chemistry can be characterized as multiobjective optimization (MOO) problems, due to the presence of multiple objective functions that cannot be easily merged into a single metric. The objective functions are typically conflicting, so that MOO problems do not have a single solution that is optimal for all objectives simultaneously. Instead, a set of points, each of which corresponds to a trade-off between the objectives, is sought, such that an improvement in one objective can only be achieved through a sacrifice in another (Miettinen, 1998). These points are commonly known as Pareto-optimal solutions (or Pareto points, or nondominated points). In most practical applications, it is not possible to derive an analytical expression that describes the loci of these points in the space of the objective functions (the Pareto frontier) (Deb, 2001). As a result, the development of MOO algorithms that can construct an approximation of the Pareto frontier efficiently is of special interest. The main criteria in the development of

*Corresponding author. E-mail addresses: c.adjiman@imperial.ac.uk

most MOO algorithms are (1) to find Pareto points within reasonable computational time and (2) to generate these points so that they are as diverse as possible and distributed evenly along the Pareto frontier.

Among the several classes of MOO solution approaches, such as stochastic methods (Zimmermann, 1978; Huang et al., 2006; Serafini, 1994), evolutionary algorithms (Li et al., 2019; Deb et al., 2000; Deb & Jain, 2013) and exact solution strategies (Belotti et al., 2013; Przybylski & Gandibleux, 2017), one of the most widely used concepts is scalarization, in which the multiple objective functions are combined into a single objective function through weight parameters and/or additional constraints, making it possible to identify solutions of the MOO problem by solving a series of single objective optimization (SOO) problems using standard optimization methods. A popular scalarization method is the weighted-sum method (Marler & Arora, 2004), in which a set of Pareto-optimal solutions is generated by varying the weights assigned to the multiple objective functions. The weighted-sum method is easy to implement and the problem is of the same degree of computational complexity as the original MOO problem since there are no additional constraints involved. However, this approach suffers from the theoretical limitations that it is not possible to capture any Pareto-optimal solutions on nonconvex regions of the Pareto frontier (Miettinen, 1998) and that an even distribution of the weights does not guarantee an even distribution of solutions on the Pareto front. The ϵ -constraint method, on the other hand, does not require any convexity assumptions on the Pareto frontier, but it has the drawback of being sensitive to the range of values of the objective functions in the feasible region, possibly resulting in infeasible or repeated Pareto-optimal solutions (Ehrgott, 2005b). Even when their range is known, the choice of ϵ values is not straightforward and it may be necessary to include additional constraints to remove regions of the feasible set. As a result, the computational cost of this approach is strongly dependent on the number of objective functions.

To deal with these shortcomings, several scalarization methods have been proposed with a special focus on the development of a systematic way to determine scalarization parameters and to capture Pareto points from nonconvex regions of the Pareto surfaces. Kim & De Weck (2005) proposed the adaptive weighted-sum algorithm. To derive an initial representation of the Pareto frontier, the algorithm starts by generating some solution points using the weighted-sum method with a (large) uniform step size in the weighting coefficients. Thereafter, the algorithm continues to solve the weighted-sum scalarization with additional upper bounds on the objective functions for the regions that need further refinement. These regions are determined by computing the distance between neighboring solutions, to control the distribution and uniformity of the Pareto points. With this method, it is possible to investigate nonconvex regions of the Pareto front. Furthermore, the approach provides a systematic way of obtaining more uniformly distributed Pareto points. However, the algorithm can generate dominated solutions and it cannot be guaranteed to cover the entire set of nondominated points.

Das & Dennis (1998) introduced the normal boundary intersection (NBI) method for identifying the solutions of nonconvex MOO problems. The method generates a well-spaced set of points on the boundary of the space of objective function values by iteratively solving a scalarized subproblem with respect to reference points placed on the convex hull of the individual minima (CHIM) of the objectives. In contrast to weighted-sum methods where problem size is preserved in the subproblems, a new vector of equality constraints is introduced, resulting in a size increase. The performance of the method was tested for large-scale and highly constrained optimization problems in the area of optimal control (Logist et al., 2010). While the method was found to produce evenly distributed solutions, its focus is on identifying the boundary of the feasible objective space, which may include some points dominated by others. Furthermore, it may be difficult to achieve convergence when there is no feasible solution that satisfies the equality constraints for the given choice of scalarization parameter values.

Following similar concepts, [Ismail-Yahaya & Messac \(2002\)](#) proposed the normal constraint (NC) method as an alternative to the NBI method to avoid getting dominated solutions and improve convergence behavior. Instead of introducing equality constraints in the subproblems, as in the NBI method, a set of inequality constraints is used to reduce the size of the feasible region. [Messac et al. \(2003\)](#) further modified the NC method by incorporating a so-called Pareto filter, which is used to eliminate non-Pareto-optimal solutions. However, these normal constraint methods share the same drawbacks as the NBI method because they rely on the CHIM as a reference line or plane. Further adjustments were made by [Messac & Mattson \(2004\)](#) and [Shao & Ehrgott \(2007\)](#), with the aim of reducing the likelihood of missing regions of the nondominated set. [Messac & Mattson \(2004\)](#) used an extension of the reference plane defined by the CHIM, so that the entire Pareto set can be enclosed by a hypercube. These studies indicate that non-connectivity of the Pareto surface and the presence of isolated Pareto-optimal points can cause severe problems for the NBI method, whereas the WS and NC methods are less likely to be affected by the disconnected nature of the Pareto set. In further work on the NBI method, [Shao & Ehrgott \(2016\)](#) suggested an extension of an approach initially designed for the solution of multiobjective linear programming (MOLP) problems ([Shao & Ehrgott, 2007](#)), in which they combined the global shooting method ([Benson & Sayin, 1997](#)) with the NBI method to guarantee coverage of the Pareto frontier as well as an even distribution of the Pareto points.

While the methods discussed so far are designed to identify evenly distributed points on the Pareto frontier, the development of Benson’s outer approximation algorithm ([Benson, 1998](#)) has motivated the emergence of another class of algorithms designed to generate outer and/or inner approximations of the Pareto frontier. The majority of such methods have been focused on obtaining polyhedral approximations to ensure an even spread of points over the Pareto surface. [Shao & Ehrgott \(2008\)](#) and [Ehrgott et al. \(2011\)](#) presented improvements to Benson’s algorithm for the solution of MOLP problems by introducing the sandwich (SD) algorithm so that the Pareto frontier is located between the inner and outer approximations. The SD algorithm and its variants have several useful properties. As the real Pareto surface is sandwiched between the inner and outer approximation, an upper bound on the approximation error can be calculated; this provides valuable information on the accuracy of the Pareto-optimal solutions generated during the course of the algorithm. Furthermore, the approximation quality can be improved efficiently by adding more solutions to the region where the error bound is largest. However, the method is limited to MOLP problems and cannot easily be applied to general convex MOO problems. Modified versions of the SD algorithm were proposed by [Solanki et al. \(1993\)](#); [Craft et al. \(2006\)](#); [Rennen et al. \(2011\)](#); [Klamroth et al. \(2003\)](#); [Bokrantz & Forsgren \(2013\)](#) to address general convex MOO problems. [Solanki et al. \(1993\)](#) extended the SD algorithm to make it applicable to higher dimensions of the MOLP problems. At each iteration, a weighted-sum subproblem is solved for the facet that exhibits the largest distance to a point constrained to the outer approximation. Within the algorithm, the accuracy of the Pareto front approximation is improved by recursively constructing inner and outer approximations through the generation of a convex hull and the identification of supporting hyperplanes. Although this method is directed towards the solution of MOLP problems, it can also be applied to general convex MOO problems. [Klamroth et al. \(2003\)](#) used two separate algorithms for generating the inner and outer approximations of the Pareto set and combined them by alternatively solving one iteration of each algorithm without using the weighted-sum method. A major feature of their algorithm is the use of vertices as representative points to construct an inner approximation that maximizes the distance from the current inner approximation toward the outer approximation. Other authors have proposed further developments of this approach, refining the method for

calculating the error between inner and outer approximations (Craft et al., 2006) or modifying the way in which parameters are chosen (Rennen et al., 2011). Craft et al. (2006) calculated the error by considering the hyperplanes that pass through the corner points of a facet rather than by solving a linear programming problem. The next weight vector is taken from a linear combination of the weight vectors used to obtain the corner points of the facet. Rennen et al. (2011) further improved the algorithm by incorporating dummy points to ensure that all facets have a non-negative normal, which is crucial for the weighted-sum method. To reduce the computational expense, which increases exponentially with the number of objectives, Bokrantz & Forsgren (2013) suggested employing a vertex enumeration method.

While sandwich-type algorithms have provided a promising route to solving MOO problems, their applicability is often limited to convex MOO problems as they rely on weighted-sum subproblems. Accordingly, SD algorithms cannot achieve complete coverage of the regions of the Pareto frontier that are nonconvex, disconnected, or consist of discrete points.

In this study, we address these limitations by introducing a new scalarization technique and a corresponding solution algorithm, the SDNBI algorithm, for the accurate approximation of nonconvex and combinatorial Pareto fronts in bi-objective optimization (BOO) problems. Such problems may contain nonconvex functions and involve a mixed set of continuous and integer decision variables. The development of the approach is focused on the interplay between the NBI method and the SD algorithm, exploiting the strengths of both. We present three main modifications, in particular making use of the modified NBI (mNBI) method suggested by Shukla (2007), and we investigate their theoretical properties: 1) the validity of the inner and outer approximations derived from the solution of the scalarized subproblem and convex hull generation, 2) the completeness of decomposing of an objective search space based on the convexity of the Pareto front, and 3) the effectiveness of modifying the subproblems in avoiding unnecessary search steps around the disconnected or isolated portions of the Pareto front. To assess the performance of the proposed SDNBI algorithm, numerical tests are conducted for five bi-objective benchmark problems (MOP1, SCH2, TNK, ZDT3, and ZDT5) and compared with the results produced by the original SD algorithm and the mNBI method. The performance of the different algorithms is compared based on reliability and efficiency criteria. While not presented in this paper, it is worth noting that an early version of the SDNBI algorithm has also been successfully applied to challenging molecular-design problems, demonstrating its broader applicability and potential (Lee et al., 2020).

The remainder of this article is organized as follows. In section 2, all relevant preliminaries including the notation, definitions and the formulation of the problems are introduced. In section 3, we describe the NBI, mNBI and SD algorithm and their properties. In section 4, we propose the new algorithm and highlight its characteristics. We perform numerical experiments in Sections 5 and 6 to investigate algorithmic efficiency. Finally, we state the main conclusions, also including future perspectives for this research in Section 7.

2. Preliminaries

The generic mathematical formulation of the MOO problem is defined as:

$$\begin{aligned} & \text{minimize} && f_1(\mathbf{x}), \dots, f_m(\mathbf{x}) \\ & \text{subject to} && \mathbf{x} \in X := \{\mathbf{x} \in \mathbb{R}^{n_1} \times \mathbb{N}^{n_2} \mid \mathbf{g}(\mathbf{x}) \leq \mathbf{0}, \mathbf{h}(\mathbf{x}) = \mathbf{0}\}, \end{aligned} \tag{MOP}$$

where $f_j : \mathbb{R}^n \rightarrow \mathbb{R}$, $j = 1, 2, \dots, m$, are the m objective functions, \mathbf{x} is an n -dimensional vector of variables ($n = n_1 + n_2$), which consists of n_1 continuous variables and n_2 integer variables, $X \neq \emptyset$ is a nonempty feasible set, $\mathbf{g}(\mathbf{x})$ is a p -dimensional vector of inequality constraints and $\mathbf{h}(\mathbf{x})$ is a q -dimensional vector of equality constraints, $q \leq n$. we assume that all $f_j(\mathbf{x})$, $j = 1, 2, \dots, m$, are bounded by some upper bound $U \in \mathbb{R}$ and lower bound $L \in \mathbb{R}$ for any instance of the MOO problem. Note that we use \mathbb{R} to denote the set of real numbers, \mathbb{R}_+ to denote the set of non-negative real numbers, and \mathbb{R}_{++} to denote the set of positive real numbers. We consider problems for which a constraint qualification holds so that the Karush-Kuhn-Tucker (KKT) optimality conditions apply when the discrete variables are relaxed or fixed, i.e., nonlinear programming (NLP) problems.

When the objective functions conflict with each other, no single solution can simultaneously minimize all scalar objective functions. Therefore, it is necessary to introduce a new notion of optimality or Pareto efficiency (Ehrgott, 2005a).

Definition 1. The *objective space* is defined as the set of all feasible combinations of the objective function values, i.e., $Z = \{\mathbf{f}(\mathbf{x}) \mid \mathbf{x} \in X\}$

Definition 2. A point $\mathbf{x}^* \in X$ is called *weakly efficient* (or *weakly Pareto-optimal*) if there exists no feasible point $\mathbf{x} \in X$ such that $f_j(\mathbf{x}) < f_j(\mathbf{x}^*)$ for all $j = 1, \dots, m$. A point $\mathbf{x}^* \in X$ is called an *efficient solution* (or *Pareto-optimal*) if there exists no feasible point $\mathbf{x} \in X$ such that $f_j(\mathbf{x}) \leq f_j(\mathbf{x}^*)$ for all $j = 1, \dots, m$, and $f_{j'}(\mathbf{x}) < f_{j'}(\mathbf{x}^*)$ for at least one $j' \in \{1, \dots, m\}$. If \mathbf{x}^* is an efficient solution, the point in objective space $\mathbf{z} = \mathbf{f}(\mathbf{x}^*)$ is referred to as a *nondominated solution* or *Pareto point* in the objective space Z .

Definition 3. (Marler & Arora, 2004) The set of efficient solutions Ω^* is the *complete set of efficient solutions* if it contains all possible efficient solutions \mathbf{x}^* . The set Ψ^* is the *efficient frontier* (or *Pareto front*) formed by all nondominated solutions, $\Psi^* = \{\mathbf{f}(\mathbf{x}^*) \mid \mathbf{x}^* \in \Omega^*\}$.

Definition 4. (Marler & Arora, 2004) Any subset of the set of efficient solutions $\mathbf{X}_E \subset \Omega^*$ is an approximation of the complete set Ω^* and has a corresponding approximation of the efficient frontier $\mathbf{Z}_E = \{\mathbf{f}(\mathbf{x}^*) \mid \mathbf{x}^* \in \mathbf{X}_E\}$. Note that $\mathbf{Z}_E \subset \Psi^*$.

Definition 5. The ideal objective vector or utopia point \mathbf{f}^{id} is defined as the objective vector whose components are the optimal objective function values of each single-objective problem, i.e., $f_j^{id} = \min_{\mathbf{x} \in \Omega^*} f_j(\mathbf{x})$, $j = 1, \dots, m$. The objective vector \mathbf{f}^{nd} is defined as the nadir objective vector and is such that $f_j^{nd} = \max_{\mathbf{x} \in \Omega^*} f_j(\mathbf{x})$, $j = 1, \dots, m$.

Definition 6. Let $\mathbf{x}^* \in \mathbf{X}_E$. If there is a vector $\boldsymbol{\lambda} \in \mathbb{R}_{++}^m$ such that \mathbf{x}^* is an optimal solution to $\min_{\mathbf{x} \in X} \boldsymbol{\lambda}^\top \mathbf{f}(\mathbf{x})$, then \mathbf{x}^* is called a *supported efficient solution* and $\mathbf{z} = \mathbf{f}(\mathbf{x}^*)$ is called a *supported nondominated objective vector*.

Definition 7. A set of Pareto points is said to be *convex*, if all nondominated points $\mathbf{z} \in \Psi^*$ are on the boundary of the convex envelope of \mathbf{Z} , which is the smallest convex set that contains \mathbf{Z} .

Note this does not imply that the Pareto front is continuous, but rather it is a relaxed interpretation of *convexity* introduced to distinguish between a supported and an unsupported nondominated objective vector. Only supported nondominated points are attainable by means of a weighted-sum scalarization approach.

3. Background and Motivation

We start with a short recapitulation of the two MOO algorithms that motivate the new algorithm proposed in the current work.

3.1. Sandwich Algorithm

The SD algorithm proposed by Solanki et al. (1993) is a scalarization method developed aimed at approximating a (convex) Pareto front while solving as few optimization subproblems as possible. While there are variations of the approach, SD algorithms are based on the successive solution of weighted-sum subproblems in which the multiple objective functions are aggregated into a single objective function using a weight vector, \mathbf{w} , as follows:

$$\min_{\mathbf{x} \in X} \quad \mathbf{w}^\top \mathbf{f}(\mathbf{x}) = \sum_{i=1}^m w_i f_i(\mathbf{x}). \quad (\text{WSP}\mathbf{w})$$

The key concepts necessary to describe an SD algorithm are set out in this section by adopting the definitions and notation of Remmen et al. (2011). A detailed description of the algorithm, including figures and a pseudo-algorithm, is provided in the Supplementary Materials (see Section S1 therein).

Definition 8. *Anchor point* – Anchor point \mathbf{z}^{Ai} is a point in objective space equal to the optimal objective function vector obtained by solving problem (WSP \mathbf{w}) with weight vector \mathbf{w}^i such that $w_i^i = 1 - \delta$ and $w_j^i = \delta$, $j = 1, \dots, m$, $j \neq i$, where δ is a small positive infinitesimal scalar value. Thus $\mathbf{z}^{Ai} = \mathbf{f}(\mathbf{x}^*)$, where $\mathbf{x}^* = \operatorname{argmin}_{\mathbf{x} \in X} \mathbf{w}^{i\top} \mathbf{f}(\mathbf{x})$.

Definition 9. *Hyperplane* – A hyperplane in the objective space is given by $H(\mathbf{w}, b) = \{\mathbf{z} \in Z \mid \mathbf{w}^\top \mathbf{z} = b\}$ with $\mathbf{w} \in \mathbb{R}^m \setminus \{\mathbf{0}\}$ and $b \in \mathbb{R}$.

Remark 1. The vector \mathbf{w} is a normal to the hyperplane. In this paper, the vector \mathbf{w} is always taken to be a unit normal vector, such that $\|\mathbf{w}\| = 1$.

A half-space and the inner normal are defined as follows.

Definition 10. *Half-space* – The set $HS(\mathbf{w}, b) = \{\mathbf{z} \in \mathbb{R}^m \mid \mathbf{w}^\top \mathbf{z} \geq b\}$ is the half-space.

Remark 2. The vector \mathbf{w} , $\|\mathbf{w}\| = 1$, is an *inner unit normal* of the half-space.

Definition 11. *Supporting hyperplane of a convex set* – Suppose C is a convex set and \mathbf{z}_0 is a point that lies on the boundary of C , $\mathbf{bd} C$, i.e., $\mathbf{z}_0 \in \mathbf{bd} C$. If $\mathbf{w} \neq \mathbf{0}$ satisfies $\mathbf{w}^\top \mathbf{z} \geq \mathbf{w}^\top \mathbf{z}_0$ for all $\mathbf{z} \in C$, then a hyperplane $H(\mathbf{w}, b)$ defined by $\mathbf{w}^\top \mathbf{z} = b$, where $b = \mathbf{w}^\top \mathbf{z}_0$, is called a *supporting hyperplane* to C at point \mathbf{z}_0 . This is equivalent to saying that the hyperplane $H(\mathbf{w}, b)$ supports C at \mathbf{z}_0 .

Definition 12. *k-face, facets and extreme points* – A set of points F of dimensionality k is a k -face of C if there exists a hyperplane $H(\mathbf{w}, b)$ that supports C at \mathbf{z}_0 and for which it holds that $H(\mathbf{w}, b) \cap C = F$. If $C \subseteq \mathbb{R}^m$, its $(m - 1)$ -faces are the facets F_S and its 0-faces are the extreme points (vertices).

For $m = 2$, we denote a p -th facet which is defined with two extreme points \mathbf{z}^{p1} and \mathbf{z}^{p2} as $F_S^p(\mathbf{z}^{p1}, \mathbf{z}^{p2})$, where it holds $\mathbf{z}_1^{p1} < \mathbf{z}_1^{p2}$. A graphical interpretation of supporting hyperplanes, half-spaces, $(m - 1)$ -faces, and 0-faces in two-dimensional space is given in Figure S1 in the Supplementary Materials.

Definition 13. *Inner and outer approximations* – A set $IPS \subseteq Z$ is an inner approximation of Ψ^* if it satisfies:

$$\forall \mathbf{z}' \in IPS, \exists \mathbf{z} \in \Psi^* : \mathbf{z}' \geq \mathbf{z},$$

where the inequality is understood component-wise. Similarly, a set $OPS \subseteq \mathbb{R}^m$ is an outer approximation of Ψ^* if it satisfies:

$$\forall \mathbf{z}' \in OPS, \exists \mathbf{z} \in \Psi^* : \mathbf{z}' \leq \mathbf{z}.$$

The SD algorithm iteratively refines inner and outer approximations of the Pareto front. The inner approximation is formed via a convex hull, while the outer approximation is generated through weighted-sum subproblems. These approximations progressively sandwich the Pareto front, improving with each iteration. The process continues until the maximum approximation error, d_{max} , which measures the distance between the inner and outer approximations, is less than a predefined tolerance ϵ . The error d_{max} is calculated as the largest facet-specific error, $d_{error,p}$, as defined by Equations (S2) and (S3). The major advantage of this method is that the weight vectors are systematically chosen to be normal to the facets generated by the inner approximation and the accuracy of the approximation is measured during the course of the algorithm, providing a natural stopping criterion.

3.2. Normal Boundary Intersection

The original NBI method was proposed by [Das & Dennis \(1998\)](#) to generate uniformly distributed boundary points for a nonlinear multiobjective optimization problem, as illustrated in Figure S3(a). To further ensure Pareto-optimality of all solutions, [Shukla \(2007\)](#) modified the method using a goal-attainment approach. In the modified NBI (mNBI) method, the individual minima or anchor points are found as a first step. The CHIM is then generated as the set of all convex combinations of these individual minima. The CHIM can be expressed as $\{\Phi\beta : \beta \in \mathbb{R}_+^m, \sum_{j=1}^m \beta_j = 1\}$ where $\Phi \in \mathbb{R}^{m \times m}$ is a matrix with i^{th} column $\mathbf{z}^{Ai} - \mathbf{f}^{id}$. The mNBI subproblem (mNBI β) is formulated to search for the maximum distance t along a normal vector $\bar{\mathbf{n}}$ to the CHIM at a point defined by a specific choice of β . The resulting subproblem is described as:

$$\begin{aligned} & \max_{\mathbf{x} \in X, t} t \\ \text{s.t. } & \Phi\beta + t\bar{\mathbf{n}} \geq \mathbf{f}(\mathbf{x}) - \mathbf{f}^{id} \\ & t \in \mathbb{R}, \bar{\mathbf{n}} \in \mathbb{R}^m \end{aligned} \tag{mNBI}\beta$$

A comprehensive description of both the NBI and mNBI methods is provided in Section S2 of the Supplementary Materials, including the basic scheme of the mNBI algorithm (Algorithm S2) and a schematic illustration of the bi-objective optimization procedure (Figure S3).

3.3. Discussion

The SD algorithm has been successfully applied to several practical problems, such as the intensity-modulated radiation therapy optimization ([Craft et al., 2006](#); [Rennen et al., 2011](#)), the design of distillation processes for separating a binary mixture of chloroform and acetone ([Bortz et al., 2014](#)), the integrated design of solvents and processes ([Burger et al., 2015](#)), the design of a plate-fin heat-sink to improve economic and thermal performance ([Andersson et al., 2018](#)) and the solution of parameter estimation problems for an equation-of-state model ([Graham et al., 2022](#)), yet there are remaining difficulties to overcome. Since the SD algorithm is closely related to weighted-sum methods, unsupported solutions that lie in the nonconvex regions of the objective space cannot be attained. Thus, there is no weight vector \mathbf{w} suitable for finding an efficient solution \mathbf{x}^* in such a region.

On the other hand, the mNBI method can yield solutions that lie on the nonconvex (concave) parts of the Pareto front as well as points on the convex regions. These nondominated points can be generated with the appropriate choice of β . The efficiency of the NBI method and its variants has been investigated in the context of the optimal design of a methyl ethyl ketone production process by carrying out bi-objective optimization with an economic value and potential environmental impact as the two objectives ([Lim et al., 2001](#)), the development

of optimal bidding strategies for the participants of oligopolistic energy markets (Vahidinasab & Jadid, 2010), the design of an optimal heat exchanger that maximizes the amount of heat transfer and minimizes tube length (Siddiqui et al., 2012), and the solution of a scheduling problem for pumped hydrothermal power in which a cost function and an emission metric were considered as bi-objective criteria (Simab et al., 2018). However, unlike the SD algorithm, the mNBI method does not provide information on approximation accuracy, nor the maximum achievable approximation quality level in the presence of disconnected regions, thus making it difficult to determine when to stop the algorithm and how to choose the number of iterations N_β . These drawbacks also preclude the user from choosing the set of reference points $\Phi\beta^k \in C^{ref}$ systematically. Given the advantages derived from each algorithm and their similarity in terms of the use of convex hulls, an extension of the SD algorithm through its combination with the mNBI method is discussed in the subsequent sections.

4. Proposed Algorithm

We present here the SDNBI algorithm, a novel adaptive MOO approach for the solution of BOO problems. It is more general than the SD algorithm in that it is applicable to nonconvex problems, in particular to those with a disconnected Pareto front and feasible region. A new feature is the use of the mNBI subproblem, such that the mNBI parameters are systematically determined by the SD algorithm, in an adaptive fashion. Although the SD algorithm and the mNBI method are applicable to higher-dimensional MOO cases ($m > 2$) (Bokrantz & Forsgren, 2013), we focus here on the solution of two-dimensional (BOO) problems and adapt the terminology appropriately, as described in the following definition.

Definition 14. *Line, half-plane, tangent* – A line $H_2(\mathbf{w}, b)$ and a half-plane $HS_2(\mathbf{w}, b)$ are special cases of the hyperplane $H(\mathbf{w}, b)$ and half-space $HS(\mathbf{w}, b)$, respectively, defined for the two-dimensional objective space, $m = 2$. If a line is tangential to a curve in the bi-objective space at the point \mathbf{z}_0 , it is called a *tangent* at \mathbf{z}_0 .

4.1. Setting the parameters of the mNBI subproblem

The main idea behind the proposed SDNBI algorithm is to replace the weighted-sum subproblem that appears in the SD algorithm with the mNBI subproblem (mNBI β) so as to obtain solutions on the nonconvex part(s) of the Pareto front. Consider a facet $F_S^{p^k}(\mathbf{z}^{p1}, \mathbf{z}^{p2})$ connecting two nondominated points \mathbf{z}^{p1} and \mathbf{z}^{p2} at some iteration k . The normal vector of the facet can be used as the normal vector $\bar{\mathbf{n}}^k$ in the mNBI subproblem. Then, Φ^k is defined by the two extreme points of the facet, with its i^{th} column given by $\mathbf{z}^{pi} - \mathbf{z}^o$, $i = 1, 2$, where $\mathbf{z}^o = [\min(z_1^{p1}, z_1^{p2}), \min(z_2^{p1}, z_2^{p2})]^\top = [z_1^{p1}, z_2^{p2}]^\top$. Subsequently, the reference point $\Phi^k\beta^k$ on the facet can be determined by choosing an appropriate β^k . In this study, β^k is chosen such that the reference point $\Phi^k\beta^k$ is located at the midpoint of the facet, in order to generate a Pareto point that may be evenly placed between \mathbf{z}^{p1} and \mathbf{z}^{p2} . While in the mNBI algorithm, $\bar{\mathbf{n}}$ remains fixed throughout and the β values are chosen *a priori*, in the SDNBI algorithm, they are updated at each iteration.

4.2. Constructing valid inner and outer approximations

The solution of the mNBI subproblem at some iteration k with the proposed parameter values results in point \mathbf{z}^k that is used to update the approximations of the Pareto front. This requires careful analysis due to the potential nonconvexity of the efficient frontier. In the original SD algorithm, the outer approximation OPS is improved at iteration k by adding a line tangential to the recently identified nondominated point \mathbf{z}^k , $H_2(\mathbf{w}^k, b^k)$,

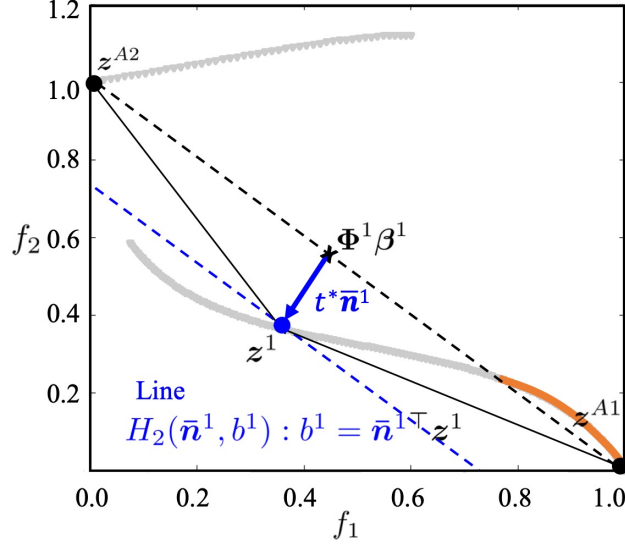


Figure 1: Illustration of a nonconvex Pareto front and the generation of an inner approximation that cuts off part of the front. The grey curve represents the boundary of the feasible region in bi-objective space for problem MOP1. The black dashed line is a facet obtained by generating a convex hull using z^{A1} and z^{A2} . The nondominated point is z^1 generated by the solution of (mNBI β) with the normal vector \bar{n}^1 and the reference point $\Phi^1 \beta^1$. The corresponding line $H_2(\bar{n}^1, b^1)$ (blue dashed line) is not tangent to the Pareto front. If the next upper bounds, i.e., inner approximations, are obtained by constructing the convex hull based on the updated set of the Pareto points, $Z_E = \{z^{A2}, z^1, z^{A1}\}$, the solid black lines are obtained, cutting off the part of the Pareto front shown in orange.

and its positive half-plane $HS_2(\mathbf{w}^k, b^k)$ where $b^k = \mathbf{w}^{k\top} \mathbf{z}^k$. The weight vector \mathbf{w}^k is used in the weighted-sum scalarization problem as described in Section 3.1. The inner approximation IPS of the Pareto front is obtained as a polyhedral approximation of the set of points $\mathbf{z} \in Z_E \subseteq \Psi^*$. This polyhedral approximation is defined as the set of all convex combinations of points in Z_E in the objective space and it is denoted by $\text{convexhull}(Z_E)$.

Thus, in the original SD algorithm, the Pareto front must be convex to ensure that valid upper and lower bounds are obtained that do not cut off any part of the front. If the Pareto front is nonconvex, the line $H_2(\bar{n}^k, b^k)$ generated as a solution of problem (mNBI β) does not necessarily support the Pareto front at point \mathbf{z}^k . A simple example where the use of the mNBI subproblem to generate a new Pareto point leads to erroneous inner and outer approximations is shown in Figure 1. It is clear that the Pareto frontier is not supported by the line $H_2(\bar{n}^1, b^1)$, where $b^1 = \bar{n}^{1\top} \mathbf{z}^1$, at nondominated point \mathbf{z}^1 . The inner approximation generated by facets $F_S^{p1}(\mathbf{z}^{A2}, \mathbf{z}^1)$ and $F_S^{p1}(\mathbf{z}^1, \mathbf{z}^{A1})$ is valid only for Pareto points $\mathbf{z}^\top = (z_1, z_2)$ in objective space such that $z_1 \leq z_1^1$. We address these issues in the remainder of this subsection.

4.2.1. Tangent at the solution of mNBI

To analyze further the properties of the mNBI subproblem, it is useful to partition the vector of variables into a continuous variable vector $\mathbf{x} \in \mathbb{R}^{n_1}$ and a binary variable vector, denoted as $\mathbf{y} \in Y = \{0, 1\}^{n_2}$. Without loss of generality, any function $q(\mathbf{x}, \mathbf{y})$ in the MOO problem, where q can refer to the objective function, an equality or an inequality constraint, can be written as

$$q(\mathbf{x}, \mathbf{y}) = \mathbf{c}_q^\top \mathbf{y} + q_x(\mathbf{x}). \quad (1)$$

Then the mNBI subproblem is given by

$$\begin{aligned} & \max_{\mathbf{x} \in X, \mathbf{y} \in Y, t} t \\ \text{s.t. } & \Phi\beta + t\bar{\mathbf{n}} \geq \mathbf{f}_x(\mathbf{x}) + \mathbf{c}_f^\top \mathbf{y} - \mathbf{f}^{id} \\ & t \in \mathbb{R}, \bar{\mathbf{n}} \in \mathbb{R}^m \end{aligned} \quad (2)$$

At the solution $(\hat{\mathbf{x}}, \hat{\mathbf{y}}, t^*)$ of the MINLP problem, one can obtain Lagrange multipliers at fixed $\mathbf{y} = \hat{\mathbf{y}}$, provided that the corresponding NLP meets an appropriate constraint satisfaction. Therefore, given an efficient solution $(\hat{\mathbf{x}}, \hat{\mathbf{y}})$ obtained by solving an mNBI subproblem and at which $t = t^*$, there exist $\boldsymbol{\mu}^*$ and $\boldsymbol{\nu}^*$ such that the KKT optimality conditions for optimization problem (2) at fixed $\hat{\mathbf{y}}$ are satisfied so that:

$$\nabla_{\mathbf{x}} \mathcal{L} = \boldsymbol{\mu}^{*\top} \nabla_{\mathbf{x}} \mathbf{f}_x(\hat{\mathbf{x}}) + \boldsymbol{\nu}^{*\top} \nabla_{\mathbf{x}} \hat{\mathbf{h}}_x(\hat{\mathbf{x}}) = \mathbf{0}, \quad (3)$$

$$\nabla_t \mathcal{L} = -1 + \boldsymbol{\mu}^{*\top} \bar{\mathbf{n}} = 0, \quad (4)$$

where $\mathcal{L}(\mathbf{x}, t, \boldsymbol{\mu}, \boldsymbol{\nu}; \hat{\mathbf{y}}) = -t + \boldsymbol{\mu}^\top (\mathbf{f}_x(\mathbf{x}) + \mathbf{c}_f^\top \hat{\mathbf{y}} - \mathbf{f}^{id} - \Phi\beta - t\bar{\mathbf{n}}) + \boldsymbol{\nu}^\top (\hat{\mathbf{h}}_x(\mathbf{x}) + \mathbf{c}_h^\top \hat{\mathbf{y}})$, $\boldsymbol{\mu} \in \mathbb{R}^m$ represents the vector of Lagrange multipliers corresponding to the augmented objective constraints $\mathbf{f}_x(\mathbf{x}) + \mathbf{c}_f^\top \hat{\mathbf{y}} - \mathbf{f}^{id} - \Phi\beta - t\bar{\mathbf{n}} \leq \mathbf{0}$, and $\boldsymbol{\nu} \in \mathbb{R}^s$ is the vector of Lagrange multipliers for the s active constraints in the set $\{\mathbf{g}_x(\mathbf{x}) + \mathbf{c}_g^\top \hat{\mathbf{y}} \leq \mathbf{0}, \mathbf{h}_x(\mathbf{x}) + \mathbf{c}_h^\top \hat{\mathbf{y}} = \mathbf{0}\}$, represented by the vector $\hat{\mathbf{h}}_x(\mathbf{x}) \in \mathbb{R}^s$, $q \leq s \leq p + q$. Furthermore, at the KKT point, the following complementarity condition must hold:

$$\boldsymbol{\mu}^{*\top} (\mathbf{f}_x(\hat{\mathbf{x}}) + \mathbf{c}_f^\top \hat{\mathbf{y}} - \mathbf{f}^{id} - \Phi\beta - t^* \bar{\mathbf{n}}) = 0. \quad (5)$$

From Equations (4) and (5), it can be deduced that at least one of the augmented objective constraints must be active. This can be shown by contradiction. Let us assume that all constraints in the augmented objective constraints are inactive, i.e., $\mathbf{f}_x(\hat{\mathbf{x}}) + \mathbf{c}_f^\top \hat{\mathbf{y}} - \mathbf{f}^{id} - \Phi\beta - t\bar{\mathbf{n}} < \mathbf{0}$ and $\boldsymbol{\mu}^* = \mathbf{0}$. Then, Equation (4) is reduced to $\nabla_t \mathcal{L} = -1 \neq 0$, which is a violation of the KKT necessary conditions. Therefore, if we solve problem (mNBI β) for any choice of parameters $(\bar{\mathbf{n}}, \beta)$, there exists a corresponding normal vector $\mathbf{w}' \geq \mathbf{0}$, where the inequality is understood component-wise, that defines a tangent to the Pareto front at the nondominated solution, \mathbf{z} , and is given by:

$$\mathbf{w}' = \frac{1}{\sum_{i=1}^m \mu_i^*} \boldsymbol{\mu}^*, \quad \sum_{i=1}^m w'_i = 1. \quad (6)$$

As Das & Dennis (1998) and Shukla (2007) have shown, an even stronger relationship between the NBI/mNBI and weighted-sum subproblems exists when the solution of the NBI/mNBI subproblem is located on a convex part of the Pareto front. A detailed discussion of this relationship is provided in Section S3 of the Supplementary Materials.

4.2.2. Decomposition of the search space

Given the line $H_2(\mathbf{w}^1, b^1)$ tangential to the Pareto front at \mathbf{z}^1 , the next step is to construct the outer and inner approximations. However, one can observe from Figure 2 that the tangent at \mathbf{z}^1 , $H_2(\mathbf{w}^1, b^1)$, intersects the nonconvex part of the Pareto front and cannot be used to generate a valid outer approximation. Similarly, the facet $(\mathbf{z}^1, \mathbf{z}^{A1})$ is below the Pareto front and cannot be used as an inner approximation. To provide valid inner and outer approximations of the Pareto front, we introduce a systematic decomposition of the search region based on the convexity of the Pareto front at the Pareto points identified, such that each Pareto-optimal

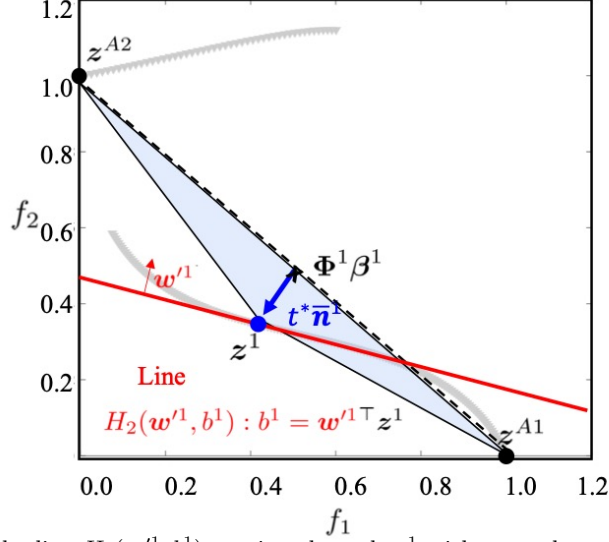


Figure 2: Representation of the line $H_2(w'^1, b^1)$ passing through z^1 with normal vector w'^1 (red solid line), calculated based on Equation (6). The grey curve represents the boundary of the feasible region in bi-objective space and the black solid lines are the facets obtained by constructing a convex hull based on the current Pareto points z^{A1} , z^{A2} and z^1 . Facet (z^1, z^{A1}) and line $H_2(w'^1, b^1)$ cannot be used to construct approximations of the Pareto front due to nonconvexity.

point z^k is supported by a line $H_2(w'^k, b^k)$ in a given space and the collection of supporting lines represents the upper or lower bounds of the Pareto front.

The idea underlying the decomposition of the search space is to divide the objective space into a number of sub-regions whenever there exist Pareto points that are exterior to the outer approximation as defined in the SD algorithm, i.e., the polyhedral set given by the supporting lines that have been derived so far.

Definition 15. *Subspace* – An l^{th} subspace $C^l(z^i, z^j)$ is a subset of bi-objective space defined by the two nondominated points z^i and z^j , where $z_1^i < z_1^j$, without loss of generality. It consists of the rectangle whose diagonal is the line segment $[z^i, z^j]$ such that all Pareto points $z = (z_1, z_2)^\top \in \Psi^*$ in the interior of the search space satisfy $z_1^i \leq z_1 \leq z_1^j$ and $z_2^j \leq z_2 \leq z_2^i$.

Definition 16. *Extreme points of a subspace* – Points z^i and z^j in subspace $C^l(z^i, z^j)$ are referred to as extreme points of the subspace.

Let $C^0(z^{A2}, z^{A1})$ denote an initial search space defined by the anchor points z^{A1} and z^{A2} , as can be seen in Figure 3. The initial set of Pareto points is $Z_E = \{z^{A1}, z^{A2}\}$. It is initially assumed that the Pareto front in C^0 is convex. By solving subproblem (mNBI β), a new nondominated point z^1 is obtained that enables one to define the corresponding supporting line $H_2(w'^1, b^1)$ and its half-plane $HS_2(w'^1, b^1)$. Note that in Figure 3, z^1 is located on the concave (or nonconvex) part of the Pareto front. The current objective space is then investigated to determine if the convexity assumption can be justified based on the current set of Pareto points. For this, we use the supporting hyperplane theorem, a proof of which can be found in Luenberger (1997):

Theorem 4.1. *Supporting hyperplane theorem* – Suppose $C \subseteq \mathbb{R}^m$ is a nonempty convex set and z_0 is a point on its boundary $\text{bd}(C)$, i.e., $z_0 \in \text{bd}(C)$. Then, there exists a supporting hyperplane $\{z \mid w'^\top z = w'^\top z_0\}$ such that $w'^\top z \geq w'^\top z_0$ for all $z \in C$, $z \neq 0$.

Corollary 4.1.1. Suppose convex set $V \subseteq C \subseteq \mathbb{R}^m$, where $m = 2$, is a polyhedron defined by a finite number of half-planes and lines $V = \{z \mid w'^k \top z \geq w'^k \top z^k, k = 1, \dots, n\}$. If each point z^k is supported by line $H_2(w'^k, b^k)$ where $b^k = w'^k \top z^k$, then every point $z \in V$ must satisfy $w'^k \top z \geq b^k$ for all $k = 1, \dots, n$.

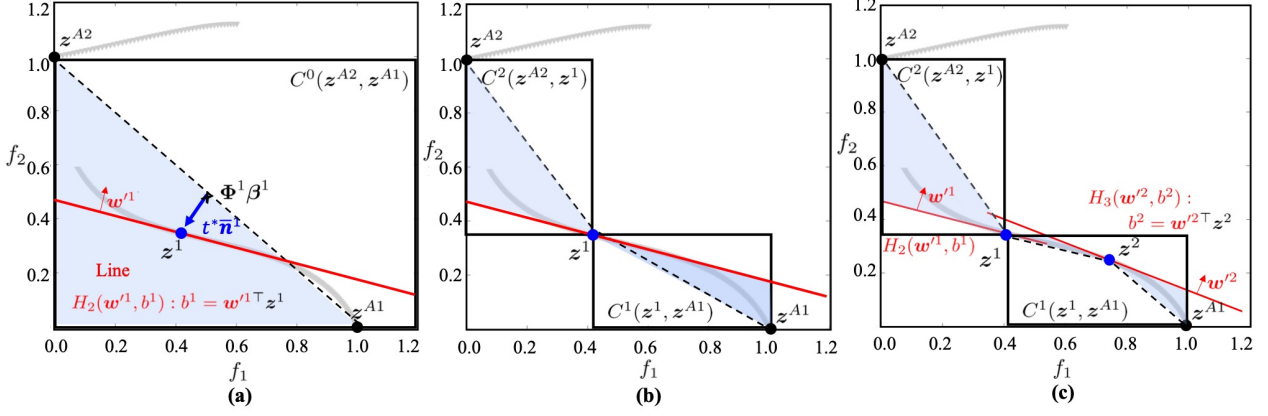


Figure 3: Schematic illustrating the procedure for the decomposition of the bi-objective space in the case of a nonconvex Pareto front, with boundary points of the feasible region shown with grey symbols (\bullet): (a) An initial objective space is characterized by subspace $C^0(z^{A2}, z^{A1})$ (black rectangular box), assumed to contain a convex Pareto front. A new nondominated point z^1 is found by solving problem (mNBI β) for $\Phi^1 \beta^1$; (b) the initial objective space is decomposed into subspaces $C^1(z^1, z^{A1})$ and $C^2(z^{A2}, z^1)$ that are assumed to contain nonconvex and convex Pareto fronts, respectively. The inner approximation of the Pareto front in C^2 is the facet (z^{A2}, z^1) (black dashed line) and the outer approximation is given by the segment of the tangent at z^1 (red solid line) connecting z^1 to the $f_1 = 0$ line and by the $f_1 = 0$ line. For subspace C^1 , the inner approximation is given by the segment of the tangent at z^1 (red solid line) connecting z^1 to the $f_1 = 1$ line and by the $f_1 = 1$ line, while the outer approximation is given by the facet (z^1, z^{A1}) ; (c) the approximation of the Pareto front is improved by adding z^2 and the subspace C^1 is not decomposed since $w'^2 z \leq b^2$ holds for all $z \in Z_E^{C^1}$. For subspace C^1 , the inner approximation is given by the segment of the tangent at z^2 (red solid line), while the outer approximation is given by the convexhull (z^1, z^2, z^{A1})

It can be observed in Figure 3(a) that both inner approximation and outer approximation are not valid, cutting off the Pareto front. The nondominated point z^{A1} does not satisfy $w^{1\top} z^{A1} \geq b^1$, implying that z^{A1} is located on a nonconvex part of the Pareto front in the subspace of C^0 . On the other hand, the nondominated point z^{A2} satisfies $w^{1\top} z^{A2} \geq b^1$ so that the hyperplane can be assumed to be supporting in the subspace $C^2(z^{A2}, z^1)$. Subsequently, the search region is decomposed, as shown in Figure 3(b), into $C^2(z^{A2}, z^1)$, with the assumption that the Pareto front is convex in this subspace, and $C^1(z^1, z^{A1})$, with the assumption that the Pareto front is nonconvex in this subspace. For any subspaces that fall under a convexity assumption, the inner approximation and outer approximation are obtained as described in Section 3.1, following the SD algorithm. By contrast, for subspaces that fall under a nonconvexity assumption, the inner approximation is constructed using the supporting lines of the nondominated points in the subspace, $IPS = \{z \mid W'^\top z \geq B'\}$, where w' is a matrix with each column corresponding to a particular normal vector w'^k and B' is a column vector where the k -th element is obtained by the vector product between the transpose of the k -th column of w' and the corresponding nondominated solution z^k . The outer approximation is constructed as the convex hull of the nondominated points in the subspace. The addition of a further Pareto point z^2 in subspace C^1 is shown in Figure 3(c) and does not require further decomposition of this subspace.

The decomposition strategy can be generalized as follows:

1. Consider a search subspace $C^l(z^i, z^j)$ in which the Pareto front is assumed to be convex, an associated set of known nondominated points, $Z_E^{C^l}$, and a newly identified nondominated point z^* within the subspace, with the corresponding line $H_2(w'^*, b^*)$, where $b^* = w'^{* \top} z^*$. If $w'^{* \top} z \geq b^*$ holds for all $z \in Z_E^{C^l}$, add z^* to $Z_E^{C^l}$ and retain the convexity assumption on subspace C^l .
2. Consider a search subspace $C^l(z^i, z^j)$ in which the Pareto front is assumed to be nonconvex, an associated set of known nondominated points, $Z_E^{C^l}$, and a newly identified nondominated point z^* within the

subspace, with corresponding line $H_2(\mathbf{w}^*, b^*)$, where $b^* = \mathbf{w}^{*\top} \mathbf{z}^*$. If $\mathbf{w}^{*\top} \mathbf{z} \leq b^*$ holds for all $\mathbf{z} \in \mathbf{Z}_E^{C^l}$, add \mathbf{z}^* to $\mathbf{Z}_E^{C^l}$ and retain the nonconvexity assumption on subspace C^l .

3. If the conditions in 1 and 2 are violated, then partition subspace C^l into two or more subspaces by investigating all nondominated points, $\mathbf{z} \in \mathbf{Z}_E^{C^l} \cup \{\mathbf{z}^*\}$. N^l new subspaces are created based on the supporting hyperplane theorem, such that $\bigcup_{dc=1}^{N^l} C^{l,dc} = \mathbf{Z}_E^{C^l} \cup \{\mathbf{z}^*\}$ and for each $dc = 1, \dots, N^l$, $C^{l,dc}$ must be such that:

$$\hat{\mathbf{w}}^\top \mathbf{z} \geq \hat{\mathbf{w}}^\top \hat{\mathbf{z}} \text{ for all } \mathbf{z}, \hat{\mathbf{z}} \in C^{l,dc}, \quad (7)$$

or

$$\hat{\mathbf{w}}^\top \mathbf{z} \leq \hat{\mathbf{w}}^\top \hat{\mathbf{z}} \text{ for all } \mathbf{z}, \hat{\mathbf{z}} \in C^{l,dc}. \quad (8)$$

where $\hat{\mathbf{w}}$ is the vector associated with nondominated point $\hat{\mathbf{z}}$.

The number of subspaces is chosen to be as small as possible while meeting the supporting hyperplane criteria. A convexity (respectively nonconvexity) assumption is made on the Pareto front in a subspace $C^{l,dc}$ if Equation (7) (respectively Equation (8)) holds.

4.3. Identification of disconnected regions of a Pareto front

One important aspect of the SDNBI algorithm is its ability to increase the likelihood of finding a new Pareto point by avoiding convergence to a boundary point. However, the mNBI method may be inefficient when a Pareto front consists of many disconnected regions or in the extreme case when it consists of a finite set of points, i.e., for a purely integer problem. This is because the portion of the objective space that can be explored by the mNBI method is limited by the choice of parameters $(\bar{\mathbf{n}}, \boldsymbol{\beta})$. If the search direction defined by these parameters does not lead to a region where as-yet-unknown nondominated points exist, the algorithm will converge to a previously identified nondominated solution, making it difficult to determine a new search direction. As a result, the algorithm may not identify Pareto points efficiently for some problems, leading to a higher computational cost. For example, a case involving the repeated computation of the same nondominated point is shown in Figure 4. For a given subspace defined by $C^3(\mathbf{z}^4, \mathbf{z}^5)$, the solution of subproblem (mNBI β) for facet normal $\bar{\mathbf{n}}^6$ with reference point $\Phi^6 \beta^6$ returns the already-known nondominated point \mathbf{z}^4 . As a result, it is possible to discard the reference points belonging to the line segment defined by $\theta \mathbf{z}^4 + (1 - \theta) \Phi^6 \beta^6$, $\theta \in (0, 1)$. However, it remains difficult to ensure that further exploration will identify new nondominated points without a clear criterion for selecting appropriate mNBI parameters. In fact, as can be seen in Figure 5(b), any choice of $\boldsymbol{\beta}$ such that the reference point lies on the line segment defined by $\theta \mathbf{z}^4 + (1 - \theta) \Phi^6 \beta'^6$, $\forall 0 < \theta \leq 1$ returns the \mathbf{z}^4 . Note that \mathbf{z}^6 is obtained by solving a modified mNBI subproblem (mNBI $\bar{\mathbf{n}}(a)$), which we will discuss in the remaining part of this section and β'^6 is calculated by using the objective constraints of the NBI subproblem (NBI β) for a given parameter $\bar{\mathbf{n}}^6$ and objective function value, $\mathbf{f} = \mathbf{z}^6$.

To address this, two subproblems are introduced to fathom regions where no Pareto-optimal solutions exist. These are modifications of the original mNBI subproblem. For an arbitrary p -th facet denoted by $F_S^p(\mathbf{z}^{p1}, \mathbf{z}^{p2})$ where $z_1^{p1} < z_1^{p2}$, if the solution of subproblem (mNBI β) for given parameters $(\bar{\mathbf{n}}^k, \Phi^k \beta^k)$ lies at \mathbf{z}^{p1} , then the following subproblem is solved:

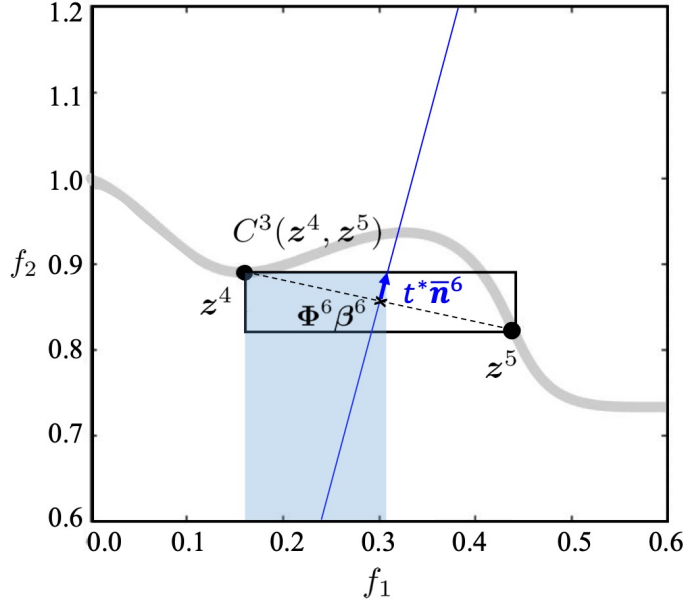


Figure 4: A geometrical illustration of the solution of the (mNBĪβ) subproblem for a disconnected Pareto front. The boundary points of the feasible region are shown with grey symbols (•). We begin by considering subspace $C^3(z^4, z^5)$ (black rectangular box). The solution of the (mNBĪβ) subproblem for facet $F_S(z^4, z^5)$ and β^6 lies at z^4 . The blue shaded region represents the area where $\Phi^6\beta^6 + t^*\bar{n}^6 \geq z^4 - f^{id}$.

$$\begin{aligned}
& \max_{x \in X, t} t \\
& \text{s.t. } \Phi^k\beta^k + t\bar{n}^k \geq f(x) - f^{id} \\
& f_1(x) \geq z_1^{p1} + \epsilon_z \\
& x \in \mathbb{R}^n, t \in \mathbb{R}, \bar{n}^k \in \mathbb{R}^m
\end{aligned} \tag{mNBĪn(a)}$$

where $z^{p1}, z^{p2} \in Z_E$ are nondominated points obtained in previous iterations, \bar{n}^k is a unit normal vector to F_S^p and ϵ_z is a small positive number.

Similarly, for the case when the solution of subproblem (mNBĪβ) lies at extreme point z^{p2} , the following subproblem is solved:

$$\begin{aligned}
& \max_{x \in X, t} t \\
& \text{s.t. } \Phi^k\beta^k + t\bar{n}^k \geq f(x) - f^{id} \\
& f_1(x) \leq z_1^{p2} - \epsilon_z \\
& x \in \mathbb{R}^n, t \in \mathbb{R}, \bar{n}^k \in \mathbb{R}^m
\end{aligned} \tag{mNBĪn(b)}$$

Theorem 4.2. Given two Pareto points z^{p1} and z^{p2} , such that $z_1^{p1} < z_1^{p2}$, and the facet $F_S^p = (z^{p1}, z^{p2})$ with normal vector \bar{n}^k , if (x^*, z^*, t^*) is a solution of subproblem (mNBĪn(a)) and z^* is a nondominated point, then there is no nondominated point $z = (z_1, z_2)^\top$ such that $z_1^{p1} + \epsilon_z < z_1 < z_1^*$. If (x^*, z^*, t^*) is a solution of a subproblem mNBĪn(b) and z^* is a nondominated point, then there is no nondominated point $z = (z_1, z_2)^\top$ such that $z_1^* < z_1 < z_1^{p2} - \epsilon_z$.

Proof. Let z^* be a nondominated point obtained at the solution (x^*, z^*, t^*) of subproblem (mNBĪn(a)) for facet $F_S^p = (z^{p1}, z^{p2})$ as defined in Theorem 4.2, with parameters $\beta^k = [\beta_1^k, 1 - \beta_1^k]$, Φ^k , and \bar{n}^k .

Suppose there exists a nondominated point z' such that $z_1^{p1} < z_1' < z_1^*$. Because z' is nondominated, there must exist a point (x', z', t') that is feasible for subproblem mNBĪn(a). Then the first inequality of subproblem

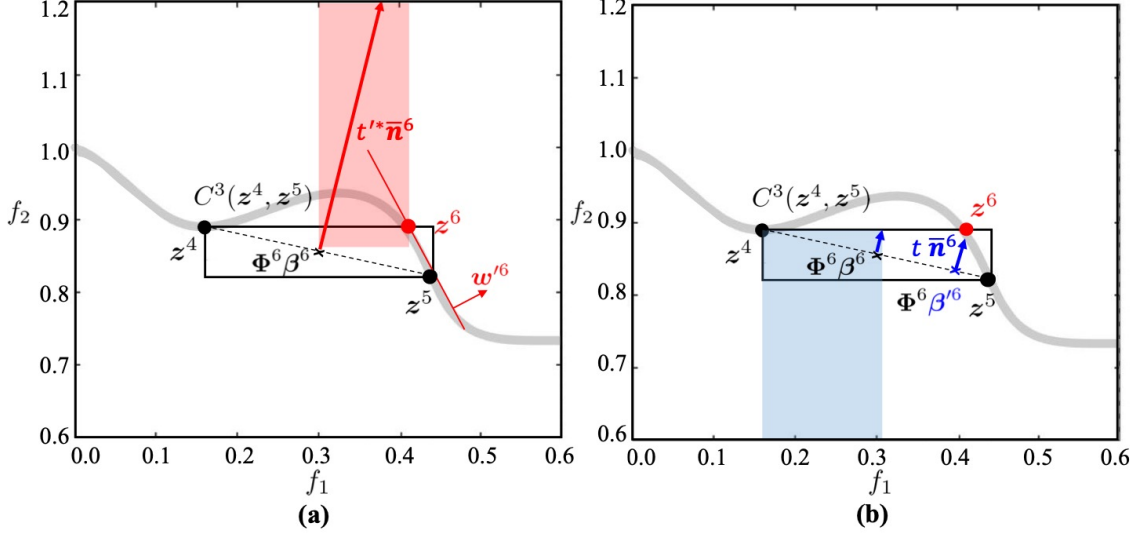


Figure 5: A geometrical illustration of the SDNBI procedure for a disconnected Pareto front when using an alternative subproblem ($\text{mNBI}\bar{n}(a)$). The boundary points of the feasible region are shown with grey symbols (\bullet). (a) A new Pareto point z^6 is generated as a solution of $\text{mNBI}\bar{n}(a)$. The red shaded region represents the area where $(\Phi^6 \beta^6 + t^* \bar{n}^6 \geq z^6 - f^{id}) \cap (z_1^6 \geq z_1^4 + \epsilon_z)$. The solid red line at z^6 represents a tangent at the solution. The facet $F_S(z^4, z^6)$ generated by an inner approximation is discarded from the search space in the subsequent iterations. In (b), it can be seen that any choice of reference points on the line segment defined by $\theta z^4 + (1 - \theta) \Phi^6 \beta^6$, $\forall 0 < \theta \leq 1$ (shown by the blue shaded region), produces the same solution z^4 .

$\text{mNBI}\bar{n}(a)$ must hold for both (x^*, z^*, t^*) and (x', z', t') :

$$\Phi^k \beta^k + t^* \bar{n}^k \geq z^* - f^{id} \quad (9)$$

$$\Phi^k \beta^k + t' \bar{n}^k \geq z' - f^{id} \quad (10)$$

By subtracting Equation (10) from Equation (9) and rearranging, we find:

$$(t^* - t') \bar{n}^k \geq z^* - z' \quad (11)$$

where \bar{n}^k is the outer-facing normal vector of the facet F_S^p and can be written as:

$$\bar{n}^k = -\Phi^k e = - \begin{bmatrix} 0 & z_1^{p2} - z_1^{p1} \\ z_2^{p1} - z_2^{p2} & 0 \end{bmatrix} \begin{bmatrix} 1 \\ 1 \end{bmatrix} = - \begin{bmatrix} z_1^{p2} - z_1^{p1} \\ z_2^{p1} - z_2^{p2} \end{bmatrix} \quad (12)$$

Therefore, the components of \bar{n}^k are always negative and the non-principal elements of Φ^k are positive. Note that the principal diagonal elements are always zero. Equation (11) is expressed component-wise as:

$$(t^* - t') \begin{bmatrix} -(z_1^{p2} - z_1^{p1}) \\ -(z_2^{p1} - z_2^{p2}) \end{bmatrix} \geq \begin{bmatrix} z_1^* - z_1' \\ z_2^* - z_2' \end{bmatrix} \quad (13)$$

Since t^* is a maximum value obtained as a solution of the problem ($\text{mNBI}\bar{n}(a)$), the strict inequality relation $t^* > t$ holds for all other feasible t . This means the components of $(t^* - t') \bar{n}^k$ are always negative. Using Equation (13), where the components in the LHS are always negative, the elements of the RHS must be negative, meaning that $z' > z^*$ holds. Since we assumed that both z^* and z' are nondominated points, there exists no feasible Pareto-optimal solution x such that $f_j(x) < z_j^*$ for all $j = 1, 2$, by Definition 2. However, this contradicts

the assumption that both \mathbf{z}^* and \mathbf{z}' are nondominated points and $z_1^{p1} < z_1' < z_1^*$. Therefore \mathbf{z}' cannot be a nondominated point and there exists no Pareto point \mathbf{z} such that $z_1^{p1} < z_1 < z_1^*$. \square

Given a Pareto front, whenever the solution of subproblem (mNBI β) for the current facet $F_S^p = [\mathbf{z}^{p1}, \mathbf{z}^{p2}]$ generates a previously identified nondominated point, the facet is further explored by solving (mNBI $\bar{n}(a)$) or (mNBI $\bar{n}(b)$), so that the empty part of the subspace can be excluded from the search space. If the solution of (mNBI $\bar{n}(a)$) or (mNBI $\bar{n}(b)$) lies at one of the Pareto points obtained in a previous iteration, the entire facet represented by $F_S^p = [\mathbf{z}^{p1}, \mathbf{z}^{p2}]$ is discarded from the search space in a subsequent iteration.

4.4. Outline of the methodology

In this section, we provide the pseudocode for the proposed SDNBI algorithm for the solution of BOO problems in Algorithm 1. The algorithm is built on the theory developed in previous sections.

In Step 1, the user specifies a convergence tolerance, ϵ , as input to the algorithm. In Step 2, key quantities are initialized: the set of known Pareto points \mathbf{Z}_E and the inner and outer approximations, IPS and OPS , respectively, are all empty. The approximation error d_{max} , the iteration counter k and the subspace counter l are also initialized. The two anchor points, \mathbf{z}^{A1} and \mathbf{z}^{A2} with $z_1^{A2} < z_1^{A1}$, are also identified. This enables the definition of the first subspace $C^0 = (\mathbf{z}^{A2}, \mathbf{z}^{A1})$, which is assumed to be convex as indicated by setting the Boolean function $Is_Convex(C^0)$ to TRUE, and of the first facet $F_S^0 = [\mathbf{z}^{A2}, \mathbf{z}^{A1}]$. There may be Pareto points in the subspace defined by this facet (i.e., in C^0) so it is considered to be “open” for further searching and the Boolean function Is_Open is set to TRUE. The set of subspaces \mathcal{C} and the set of facets \mathcal{F} are initialized. In Step 3, the facet is set to F_S^p , i.e., $p^1 = 0$.

The main loop begins at Step 4. The parameters of subproblem (mNBI β) at iteration k are specified in Step 5. Subproblem (mNBI β) is then solved in Step 6, yielding (\mathbf{z}^*, t^*) . In Steps 7 to 13, the fathoming of facet $F_S^{p^k}$ is considered as described in Section 4.3. Specifically, if \mathbf{z}^* is a member of \mathbf{Z}_E , i.e., a previously determined Pareto point, subproblem (mNBI $\bar{n}(a)$) or (mNBI $\bar{n}(b)$) is solved to generate a new (\mathbf{z}^*, t^*) . If the resulting vector \mathbf{z}^* is once more a known Pareto point, the entire facet is discarded, i.e., $Is_Open(F_S^{p^k})$ is set to FALSE.

If a new Pareto point has been found, the convexity property of the Pareto front in the current subspace C^{l^k} is examined in Steps 15-22 and new subspaces are created as required, based on Section 4.2.2. Specifically, if all the Pareto points in the subspace, $\mathbf{z} \in \mathbf{Z}_E^{C^{l^k}}$, are found to lie on the half-plane consistent with the convexity / nonconvexity assumption on C^{l^k} , then \mathbf{z}^* can simply be added to the subspace and the set of facets updated to take this new point into account. The convexity / nonconvexity of C^{l^k} is unchanged. On the contrary, if there exists at least one point in the other half-plane, the set of Pareto points $\mathbf{Z}_E^{C^{l^k}}$ is updated by adding \mathbf{z}^* and C^{l^k} is partitioned to create subspaces that only contain Pareto points that lie in the same half-space. The set of facets is updated as is the number of subspaces.

The iteration counter is then increased. The approximations IPS and OPS are updated in Step 25 and if there are no remaining facets to explore, the algorithm terminates regardless of whether the stopping tolerance has been achieved. Otherwise, the next facet $F_S^{p^k} = [\mathbf{z}^{p2}, \mathbf{z}^{p1}]$ to be explored is identified in Steps 28 and 29 as the open facet at which the largest approximation error is observed. The corresponding subspace is also identified, defined as the subspace $C^{l^k} \in \mathcal{C}$ such that $\mathbf{z}^{p2}, \mathbf{z}^{p1} \in C^{l^k}$. The algorithm terminates when the maximum approximation error is less than ϵ .

Algorithm 1 SDNBI Algorithm for bi-objective optimization

procedure SDNBI ALGORITHM

```
1: Inputs:  
   Set a quality threshold,  $\epsilon$ .  
2: Initialize:  
    $\mathbf{Z}_E = IPS = OPS = \emptyset$ ;  $d_{max} \leftarrow \infty$ ,  $k \leftarrow 1$ ,  $dc \leftarrow 0$ ,  $N_F \leftarrow 1$ .  
   Find anchor points  $\mathbf{z}^{A1}$  and  $\mathbf{z}^{A2}$  with  $z_1^{A2} < z_1^{A1}$ .  
   Define an initial search region,  $C^0(\mathbf{z}^{A2}, \mathbf{z}^{A1})$ , set  $Is\_Convex(C^0) = \text{TRUE}$  and  $\mathcal{C} = \{C^0\}$ .  
   Define facet  $F_S^0 = [\mathbf{z}^{A2}, \mathbf{z}^{A1}]$ , set  $Is\_Open(F_S^0) = \text{TRUE}$  and  $\mathcal{F} = \{F_S^0\}$ .  
3: Set  $\mathbf{Z}_E = \{\mathbf{z}^{A1}, \mathbf{z}^{A2}\}$ , set  $p^k = 0$ .  
4: while  $d_{max} \geq \epsilon$  do  
5:   Set the next normal  $\bar{\mathbf{n}}^k$  to be the outer normal to  $F_S^{p^k}$  and set the reference point  $\Phi^k \beta^k$  by choosing  $\beta^k$   
   to be the midpoint of  $F_S^{p^k}$ .  
6:   Determine  $(\mathbf{z}^*, t^*)$  by solving (mNBI $\beta$ ) with  $\Phi^k \beta^k$  and  $\bar{\mathbf{n}}^k$ .  
7:   if  $(\mathbf{z}^k \in \mathbf{Z}_E)$  then  
8:     Obtain new  $(\mathbf{z}^*, t^*)$  by solving (mNBI $\bar{\mathbf{n}}(a)$ ) or (mNBI $\bar{\mathbf{n}}(b)$ ).  
9:     if  $(\mathbf{z}^* \in \mathbf{Z}_E)$  then  
10:       Fathom facet  $F_S^{p^k}$  by setting  $Is\_Open(F_S^{p^k}) = \text{FALSE}$ .  
11:       Set  $k = k + 1$  and return to step 6.  
12:     end if  
13:   else  
14:     Define the supporting line  $H_2(\mathbf{w}'^k, b^k) : b^k = \mathbf{w}'^{k\top} \mathbf{z}^*$  using Equation (6).  
15:     if  $(Is\_Convex(\mathbf{Z}_E^{C^{l^k}}) == \text{TRUE} \text{ and } \mathbf{w}'^{k\top} \mathbf{z} \geq b^k \text{ for all } \mathbf{z} \in \mathbf{Z}_E^{C^{l^k}})$   
     or  $(Is\_Convex(\mathbf{Z}_E^{C^{l^k}}) == \text{FALSE} \text{ and } \mathbf{w}'^{k\top} \mathbf{z} \leq b^k \text{ for all } \mathbf{z} \in \mathbf{Z}_E^{C^{l^k}})$  then  
16:       Add  $\mathbf{z}^*$  to  $\mathbf{Z}_E^{C^{l^k}}$  and replace  $F_S^{p^k} \in \mathcal{F}$  by two new facets  $F_S^{p_1^k}$  and  $F_S^{p_2^k}$   
       in which  $\mathbf{z}^*$  is an extreme point. Set  $Is\_Open(F_S^{p_1^k}) = Is\_Open(F_S^{p_2^k}) = \text{TRUE}$ .  
17:     else  
18:       Update  $\mathbf{Z}_E^{C^l} = \mathbf{Z}_E^{C^{l^k}} \cup \{\mathbf{z}^*\}$   
19:       Decompose current subspace  $C^{l^k}$  into two or more subspaces by investigating  
       all nondominated points  $\mathbf{z} \in \mathbf{Z}_E^{C^{l^k}}$ , and set corresponding  $Is\_Convex$ .  
20:       Update facets for the subspaces that contain  $\mathbf{z}^*$ .  
21:       Set  $dc = dc + N^l$ , where  $N^l$  is the number of new subspaces created.  
22:     end if  
23:   end if  
24:   Set  $k = k + 1$ .  
25:   For all subspaces  $C^l \in \mathcal{C}$ ,  $l = 1, \dots, dc$ , construct  $IPS$  and  $OPS$ .  
26:   if  $(Is\_Open F_S^p == \text{FALSE}, \forall p)$  then break  
27:   end if  
28:   Compute the approximation error  $d_{error,p}$  between  $IPS$  and  $OPS$   
   for each facet  $F_S^p$  such that  $Is\_Open(F_S^p) = \text{TRUE}$ ,  $p = 1, \dots, N_F$ .  
29:   Select the facet  $F_S^{p^k}$  that presents the largest error, i.e.,  $p^k = \underset{p=1, \dots, N_F}{\operatorname{argmax}} (d_{error,p})$ ,  
   and the corresponding subspace  $C^{l^k}$ . Set  $d_{max} = d_{error,p^k}$ .  
30: end while  
end procedure
```

5. Performance of the algorithm

In this section, the numerical experiments to evaluate the performance of the proposed algorithm are discussed, and its behavior is compared with the SD algorithm and mNBI method for a set of test cases.

5.1. Test functions

To assess the performance of the three algorithms studied, five well-known problems are selected from the MOP1 (Van Veldhuizen & Lamont, 1999), ZDT (Zitzler et al., 2000), SCH (Schaffer, 1984), and TNK (Tanaka et al., 1995) test suites developed for testing evolutionary MOO algorithms. The test problems are chosen to vary in complexity in terms of problem size and numerical difficulty with convex, nonconvex and disconnected

Pareto fronts. The test problems are summarized in Table S1 of Supplementary Material where the number of decision variables n , their bounds, and the nature of the Pareto-optimal front are specified. Problem ZDT5 is a mixed-integer problem and the integer variables are denoted by the vector $\mathbf{y} \subseteq \mathbb{N}^{n_2}$, to distinguish them from the continuous variable vector, denoted by variables v_i , $i = 1, \dots, 11$, and g in this problem.

Before formulating the scalarized problems (WSP w) and (mNBI β), each objective function is normalized with respect to the limits of objective space, i.e., the ideal and nadir points, \mathbf{f}^{id} and \mathbf{f}^{nd} , to avoid biasing search direction towards a particular objective. Note that the mNBI method has been proven to be independent of the relative scales of the objective functions (Das & Dennis, 1998), but the normalization is applied to all methods in order to make a fair comparison. The m -dimensional normalized objective vector is denoted by $\hat{\mathbf{f}}$.

5.2. Performance metrics

The main goal when solving MOO problems is to generate, in the minimum time possible, a diverse set of nondominated points that are evenly distributed along the Pareto front. For nonconvex problems, there is the added challenge of ensuring that the points found are as close as possible to the true Pareto front.

Based on these considerations, we use the following performance metrics for evaluating the quality of the solution set obtained by each algorithm.

1. The number of unique non-dominated solutions (N_{unq}): N_{unq} denotes the cardinality of the set of unique Pareto points obtained in a given run, serving as a measure of the diversity of the solution set.
2. Hypervolume (HV): The hypervolume (Zitzler et al., 2003) of a set of non-dominated solutions is the volume of the m -dimensional region in objective space enclosed by the nondominated solutions obtained and a reference point, $f_{ref}, j = 1, \dots, m$. The larger HV, the better the solution set in terms of convergence to the true Pareto front and/or in terms of diversity of the solutions. In the evaluation of the hypervolume in this work, the reference point is chosen by selecting the worst (largest) value of each objective across all nondominated solutions generated by the three algorithms considered.
3. Distribution metric (DM): The distribution metric was suggested by Zheng et al. (2017) to capture the spread of the solution set over the Pareto front approximation and the extent of the true Pareto front covered by the nondominated points. This metric addresses some of the deficiencies of the metrics of Schott (1995) and Wu & Azarm (2001). Smaller values of DM indicate better distributed solution sets. The equation for DM is given by Equation (S11) in Section S4 of the Supplementary Materials.
4. CPU time: The computational time to approximate the Pareto frontier is a critical aspect for computationally expensive MOO problems. Both the total CPU time to generate all solutions ($t_{cpu,t}$) and the average CPU time taken to generate one nondominated point ($t_{cpu,a}$), defined as $t_{cpu,t}/N_{unq}$ are reported.

5.3. Implementation overview

All algorithms are implemented in Matlab 2018a using the same common subfunctions. Each subproblem derived from the scalarization method is solved through the GAMS modeling environment interfaced with CONOPT (Drud, 1994) and SNOPT (Murray, 1997; Gill et al., 2005) for nonlinear programs and DICOPT (Grossmann et al., 2002) for the mixed-integer program. Both are local solvers. All runs are performed on a single Intel(R) Xeon(R) Gold 5122 CPU @ 3.60GHz processor with 384 GB of RAM.

To increase the likelihood of identifying globally optimal Pareto points, a multi-start approach (Pál, 2013) is adopted in the solution of the subproblems. The multiple starting points (N_{sobol}) are generated via a Sobol'

Table 1: Algorithmic parameters used in the test problems

Parameter	MOP1	SCH2	TNK	ZDT3	ZDT5
N_{sobel}	20	20	20	50	30
ϵ in SDNBI	0.001	0.001	0.002	0.005	0.005
$N_{iter,fix}$	33	27	59	36	40
N_β	10	10	15	10	10
\mathbf{f}^{id}	[0.053, 1]	[7.251, 0.5]	[0.0416, 0.0416]	[0, -0.7733]	[0, 0.3226]
\mathbf{f}^{nd}	[1, 37]	[18.5, 3.045]	[1.0384, 1.0384]	[0.8518, 1]	[31, 10]

Table 2: Values of the relevant metrics for the best-known Pareto fronts of the test problems

Quality Metrics	MOP1	SCH2	TNK	ZDT3	ZDT5
N_{finite}	100	200	301	100	100
N_{unq}	100	153	200	67	31
HV (10^{-2})	92.96	63.78	30.82	51.46	89.57
DM	0.0157	0.0389	0.0238	0.0455	0.0944

sequence (Sobol’ et al., 2011) to ensure diversity in the design space. For the SD algorithm and mNBI method, the stopping criterion is defined as a fixed number of iterations $N_{iter,fix}$, selected based on the iterations taken for SDNBI to reach a pre-defined error tolerance. This is because, although the SD algorithm benefits from a stopping criterion based on a convergence tolerance, it tends to terminate early as it cannot explore nonconvex regions of the Pareto front. Furthermore, the only stopping criterion for the mNBI algorithm is related to the computational effort with no means to estimate the quality of the approximation of the Pareto front generated.

The initial set, C^{ref} , of $N_\beta - 1$ reference points for the mNBI method is chosen such that consecutive reference points $\Phi\beta^k$ and $\Phi\beta^{k+1}$ are equally spaced, with a spacing δ . This is expressed as:

$$\beta_2^k = k \times \delta, \quad \beta_1^k = 1 - \beta_2^k, \quad \text{for } k = 1, \dots, N_\beta - 1, \delta = 1/(N_\beta - 1). \quad (14)$$

Once the parameters in the initial set have been enumerated by the algorithm, the next β to be chosen, i.e., β^{N_β} is determined by taking the midpoint between two adjacent β vectors used in previous iterations of the algorithm. As previously mentioned, the values of the parameter β for the SDNBI algorithm are chosen as facet midpoints, i.e., $\beta^k = [0.5, 0.5]^\top$. All other parameters used in the numerical tests are specified in Table 1.

6. Results and discussion

In this section, we compare the performance of the SD, mNBI, and SDNBI algorithms. The “true” Pareto front and the boundary of the feasible region are generated by solving (NBI β) for MOP1, SCH2, TNK, and ZDT3 and (mNBI β) for ZDT5 using exhaustive enumeration of a large set (N_{finite}) of reference points $\Phi\beta$ in order to provide a benchmark for the quality of the solutions. The results of these calculations are referred to as the best-known approximations of the true Pareto front and used for graphical comparison. The values of relevant metrics for the best-known Pareto front obtained for each test problem are shown in Table 2. Graphical representations of the Pareto fronts and boundary points in bi-objective space are given in Figure 6.

6.1. Test problem MOP1

The results generated by applying the SD, mNBI, and SDNBI algorithms to problem MOP1 and the relative performance of the algorithms are summarized in Table 3. The algorithms are run for 33 iterations, corresponding to the convergence of the SDNBI algorithm with the chosen value of ϵ (see Table 1). For test problem MOP1,

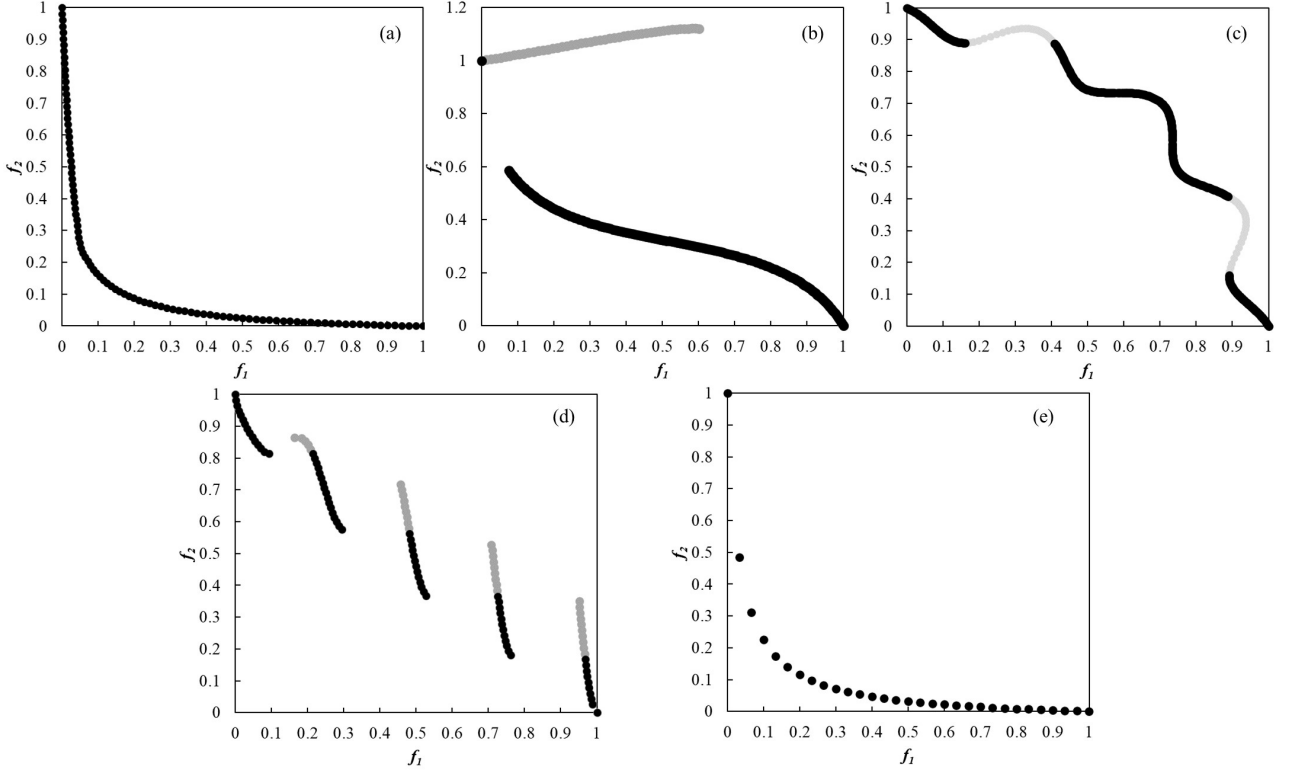


Figure 6: Best-known Pareto front (black symbols \bullet) and boundary points of the feasible region (grey symbols \bullet) in bi-objective space for the test functions: (a) MOP1, (b) SCH2, (c) TNK, (d) ZDT3, and (e) ZDT5 obtained by solving problem (NBI β) for many reference points $\Phi\beta$.

all three algorithms show similar performance in terms of HV and N_{unq} , as can be seen in Table 3. This is attributed to the convexity of the Pareto front that allows the three algorithms to generate a new nondominated point at every iteration, resulting in an equal number of Pareto points at termination. While the SD algorithm is marginally better in terms of HV, the SDNBI algorithm yields the lowest DM, indicating better-distributed solutions along the Pareto front. This can be observed in Figure 7, in which the approximate Pareto front at the 33rd iteration is shown. This better performance in DM is mainly due to the fact that in the SDNBI algorithm, the next search direction is chosen by taking into account both spacing and an approximation error: the spacing between two adjacent Pareto points is used to set the parameter β as the midpoint of a facet and the facet itself is chosen based on the distance between the inner and outer approximation, which in turn determines the value of the parameters \bar{n} and Φ , in order to minimize the error. By contrast, in the mNBI and SD algorithms, either spacing or error is considered, but not both.

Although the mNBI algorithm outperforms the SDNBI in terms of HV, it is important to note that the accuracy of the mNBI-generated approximation depends highly on the initial set of β values chosen. Yet, the number of β values required in the initial set and the number of additional values required to achieve a particular quality of solution set is unknown and there is no systematic method for determining an appropriate number. This is reflected in Figure 8(a) and 8(b) where the HV and DM values for the mNBI method exhibit the lowest initial performance. The SD and SDNBI algorithms, on the other hand, achieve high HV and low DM values that are close to the reference values (92.69 for HV and 0.0157 for DM) in few iterations, most likely because the scalarization parameters are chosen to maximize the accuracy of the approximation.

The computational cost of generating Pareto points comes at a relatively higher price for SD and SDNBI (9.2% and 5.2% higher $t_{cpu,t}$ value, cf. Table 3 and Figure 8(d) and 8(e)). The higher computational cost

Table 3: Performance metrics for the test problems MOP1 with $N_{iter,fix} = 33$ and SCH2 with $N_{iter,fix} = 27$, comparing the SD, mNBI, and SDNBI algorithms.

Problem	MOP1			SCH2		
Algorithm	SD	mNBI	SDNBI	SD	mNBI	SDNBI
N_{unq}	33	33	33	26	25	26
HV (10^{-2})	92.57	92.54	92.45	53.09	62.70	62.94
DM	0.0586	0.0534	0.0478	0.2512	0.0998	0.0910
$t_{cpu,a}$ (s)	15.05	13.78	14.49	9.35	9.46	9.41
$t_{cpu,t}$ (s)	4.97×10^2	4.55×10^2	4.78×10^2	2.43×10^2	2.36×10^2	2.44×10^2

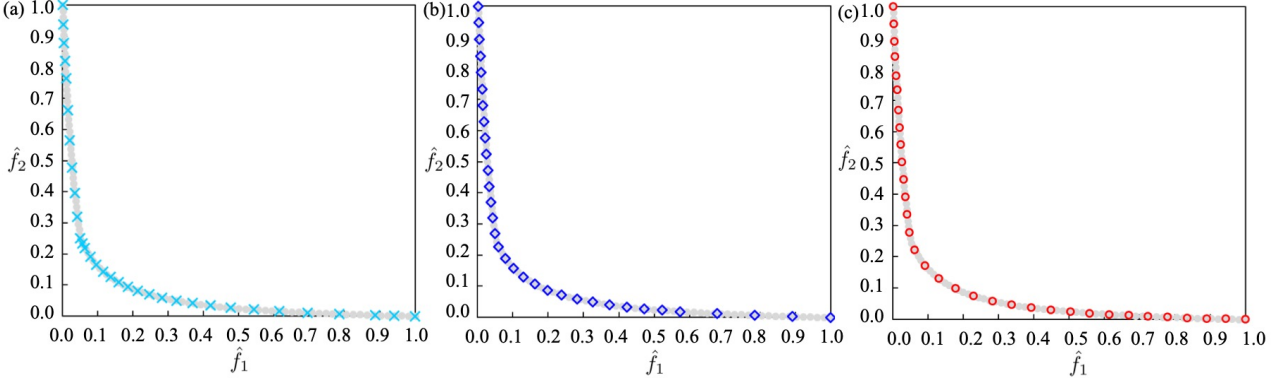


Figure 7: Pareto points generated by (a) SD (\times), (b) mNBI (Δ), and (c) SDNBI (\circ) for test problem MOP1. The best-known Pareto front is shown in grey.

is mainly associated with the time taken for convex hull generation and for linear optimization runs for the calculation of the error between the inner and outer approximations of each facet.

6.2. Test problem SCH2

Test problem SCH2 is much more challenging than MOP1 because the Pareto-optimal set consists of two disconnected regions, as shown in Figure 9. The first consists of a single point and the second is a large continuous, nonconvex region. There is a large gap between these two regions.

The desired approximation quality is achieved with the SDNBI algorithm in 27 iterations. As shown in Table 3, the highest value of HV and the lowest value of DM are achieved when using SDNBI, indicating that the nondominated points generated by SDNBI are the closest approximation to the best-known Pareto front and offer a better distribution. This can also be observed by comparing the three panels in Figure 9. It can further be seen that the points identified by the SD algorithm lie only on the convex part of the true Pareto front, as is expected, resulting in the lowest value of N_{unq} and HV, and the highest value of DM. In view of this, subsequent discussion is focused on comparing the mNBI and SDNBI algorithms.

The overall performance of the mNBI algorithm is similar to that of SDNBI in terms of HV and DM, although the mNBI algorithm trails SDNBI in early iterations (see Figure 10(a) and Figure 10(b)).

The better overall quality of the solution set obtained with SDNBI is partly as a result of recognizing discontinuities in the Pareto front. Once the corresponding facet has been fathomed, a new Pareto point can be generated at every subsequent iteration. For example, the disconnected region of the Pareto front between $0 \leq \hat{f}_1 \leq 0.07$ and also $0.59 \leq \hat{f}_2 \leq 1$ (see yellow shaded box in Figure 9) is removed from the search space at the 8th iteration by solving an alternative SDNBI subproblem ($\text{mNBI}\bar{n}(b)$). This event is also observed as a kink in the plot of N_{unq} for the SDNBI algorithm (Figure 10(c)). Fewer points are identified by the mNBI algorithm within the fixed number of iterations. This is mainly because, at several iterations, the solution of

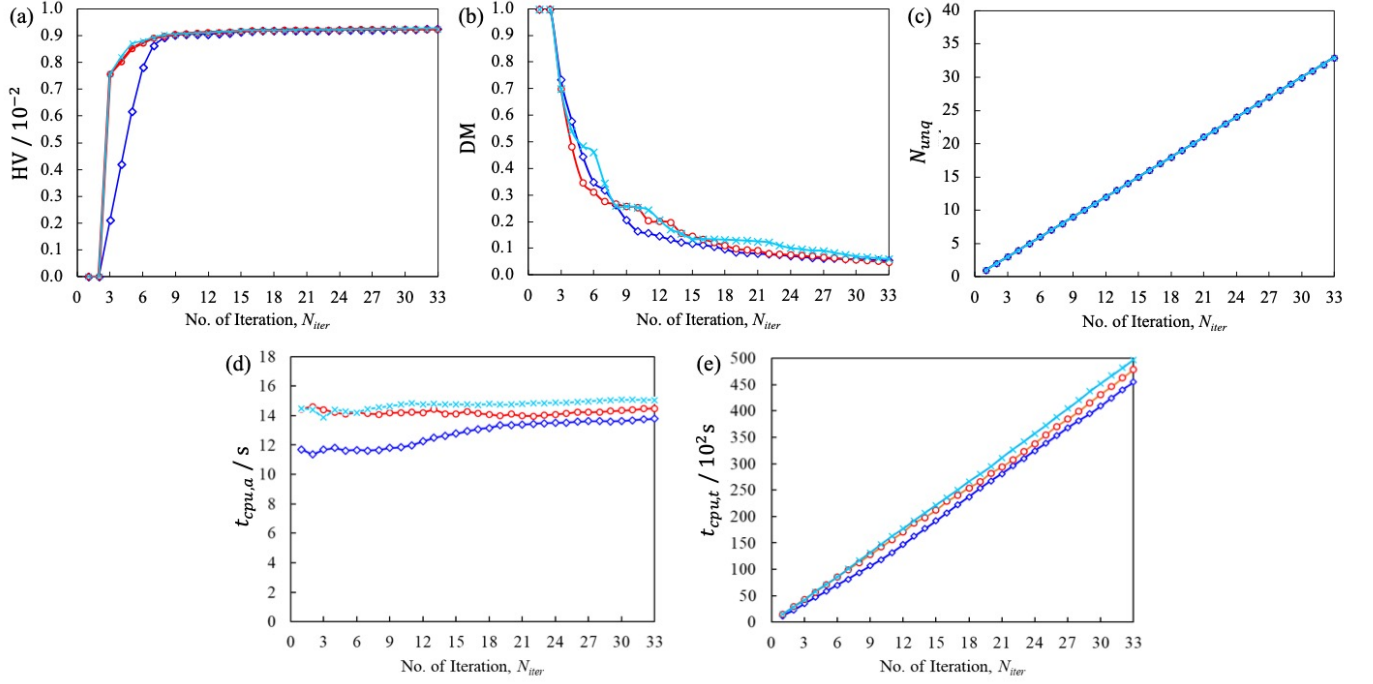


Figure 8: Performance metrics as a function of iteration number for the application of the SD algorithm (\times), mNBI algorithm (\diamond), and SDNBI algorithm (\circ) to MOP1 for 33 iterations: (a) Scaled hypervolume, HV, (b) Scaled distribution metric, DM, (c) Number of unique Pareto points, N_{unq} , (d) CPU time spent per iteration in seconds, $t_{cpu,a}$, (e) overall CPU time in seconds, $t_{cpu,t}$.

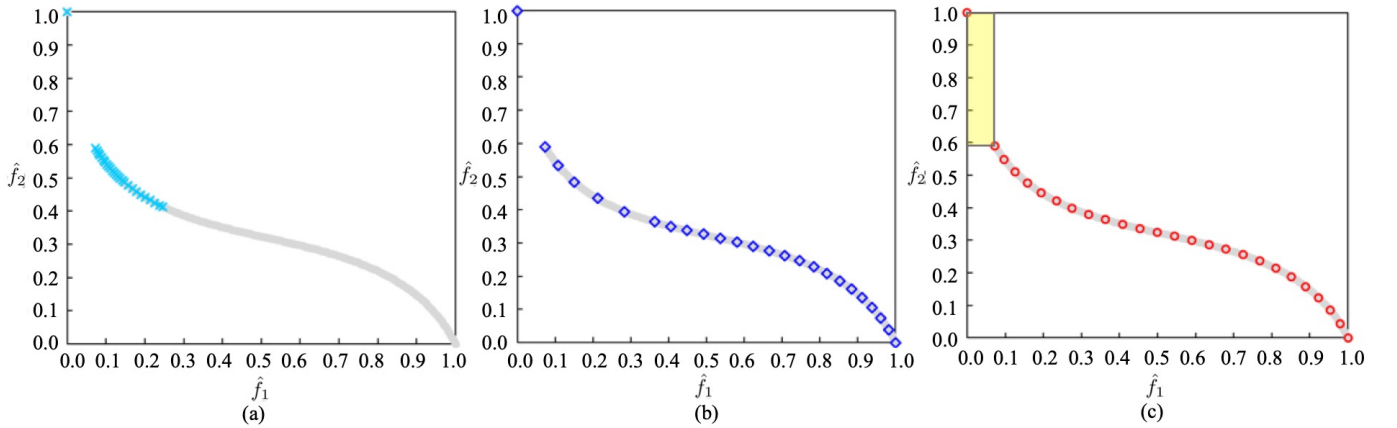


Figure 9: Pareto points generated by (a) the SD algorithm (\times), (b) the mNBI algorithm (\triangle), and (c) the SDNBI algorithm (\circ) for test problem SCH2, including the region discarded as being devoid of Pareto points (yellow shading). The best-known Pareto front is shown in grey.

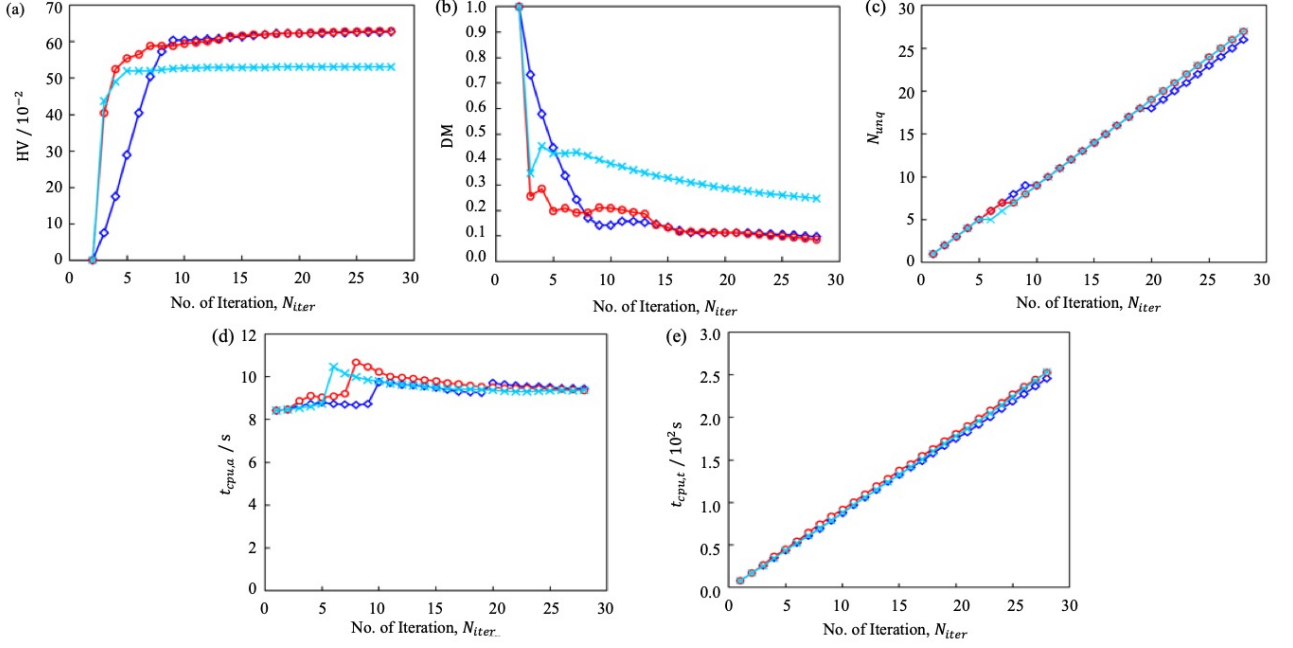


Figure 10: Performance metrics as a function of iteration number for the application of the SD ($- \times -$), mNBI ($-\diamond-$), and SDNBI ($- \circ -$) algorithms to SCH2 for 27 iterations: (a) Scaled hypervolume, HV, (b) Scaled distribution metric, DM, (c) Number of unique Pareto points, N_{unq} , (d) CPU time spent per iteration in seconds, $t_{cpu,a}$, (e) overall CPU time in seconds, $t_{cpu,t}$.

Table 4: Performance metrics for the test problems: TNK with $N_{iter,fix} = 59$, ZDT3 with $N_{iter,fix} = 36$, and ZDT5 with $N_{iter,fix} = 40$, comparing the SD, mNBI, and SDNBI algorithms. SD is omitted for TNK as it does not identify any Pareto point.

Problem Algorithm	TNK		ZDT3			ZDT5		
	mNBI	SDNBI	SD	mNBI	SDNBI	SD	mNBI	SDNBI
N_{unq}	56	59	36	35	36	23	23	31
HV (10^{-2})	30.34	30.44	48.85	51.12	51.21	89.46	89.48	89.57
DM	0.0674	0.0629	0.1356	0.0776	0.0667	0.1377	0.1230	0.0944
$t_{cpu,a}$ (s)	15.88	16.24	45.06	47.38	46.10	73.40	52.86	51.92
$t_{cpu,t}$ (s)	8.89×10^2	9.58×10^2	16.22×10^2	16.58×10^2	16.59×10^2	1688.20	1215.88	1609.64

the mNBI subproblem fails to result in a new Pareto point as searching takes place along the large disconnected region. In fact, this region is repeatedly explored during the mNBI search procedure as iterations proceed. This algorithmic behavior is illustrated in Figure 10(c), where a lower value of N_{unq} is observed with the mNBI algorithm than with the SDNBI algorithm after the 20th iteration.

Finally, all three algorithms exhibit similar performance in terms of CPU time per Pareto point and overall, as seen in Table 3 and in Figure 10(d) and 10(e). This example illustrates that with the SDNBI, it is possible to obtain a better distribution of Pareto points and to gain additional confidence that the Pareto front is described well, given the knowledge that no Pareto point exists in the relatively large discarded region.

6.3. Test problems TNK and ZDT3

Similar trends are observed for problems TNK and ZDT3 in which the nondominated sets comprise two disconnected regions for TNK and four for ZDT3, as shown in Figure 6(c) and 6(d).

A key challenge in solving these two problems is to determine a set of parameter values so that the Pareto points identified are evenly distributed and, more importantly, so that the solution of the optimization subproblems that result in convergence to an already known Pareto point is avoided.

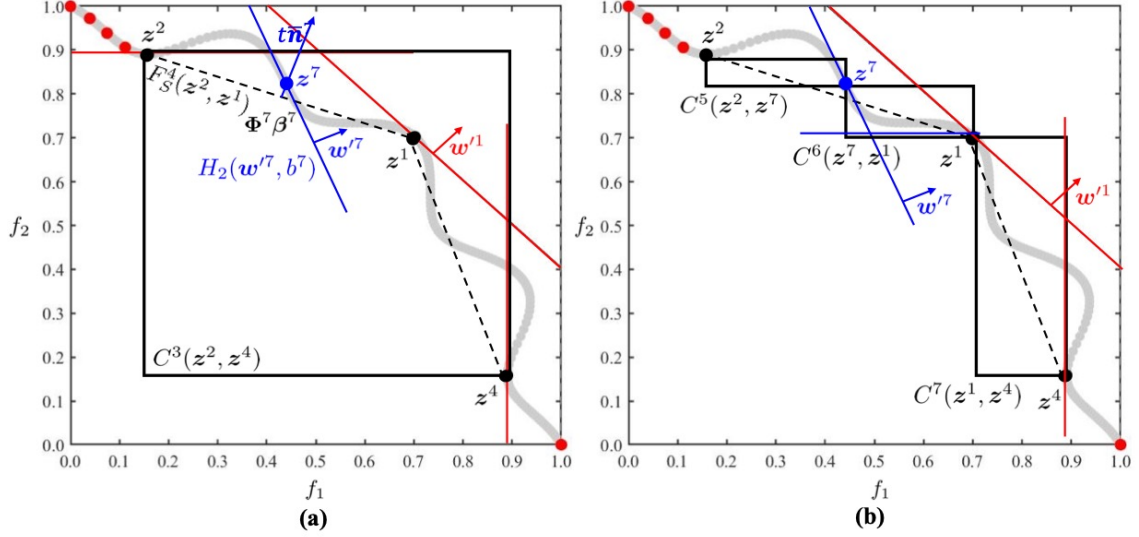


Figure 11: A geometrical illustration of the SDNBI procedure for problem TNK. (a) A new Pareto point z^7 is generated as a solution of (mNBI β) for facet F_S^4 of subspace $C^3(z^2, z^4)$ ($Is_Convex(C^3) = \text{FALSE}$). The black dashed line represents a facet obtained by $\text{convexhull}(\mathbf{Z}_E^{C^3})$. The solid red and blue lines represent supporting lines at the solutions. (b) The subspace is decomposed into three subspaces, such that all points in each subspace satisfy Equation (7) or (8). The subspaces are $C^5(z^3, z^4)$, with $Is_Convex(C^5) = \text{FALSE}$, $C^6(z^3, z^4)$, with $Is_Convex(C^5) = \text{TRUE}$, and $C^7(z^3, z^4)$, with $Is_Convex(C^5) = \text{FALSE}$, respectively.

In Figure 11, we display the 7th iteration of the SDNBI algorithm when applied to problem TNK, to exemplify how a subspace is decomposed and information on the shape or convexity of the Pareto front is obtained. At the 7th iteration, the subspace $C^3(z^2, z^4)$ is selected as containing the facet with the largest approximation error (facet $F_S^4 = [z^2, z^1]$). The subspace comprises three nondominated points, $\mathbf{Z}_E^{C^3} = \{z^2, z^1, z^4\}$ and is assumed to be nonconvex, i.e., $Is_Convex(C^3) = \text{FALSE}$. We begin by constructing inner and outer approximations as shown in Figure 11. The red lines are tangents (inner approximations) at each nondominated point and the black dashed lines represent the outer approximations generated by $\text{convexhull}(\mathbf{Z}_E^{C^3})$. The mNBI parameters $(\Phi^7 \beta^7, \beta^7)$ are selected for facet F_S^4 and the corresponding (mNBI β) subproblem is solved. From visual inspection of Figure 11(a), it is clear, given the newly generated point z^7 , $w'^{7\top} z \leq b^7$ does not hold for $z = z^1$ and $z = z^4$, indicating that the Pareto front in subspace C^3 is partly convex. Therefore, subspace $C^3(z^2, z^4)$ is decomposed into three subspaces: $C^5(z^3, z^4)$, with $Is_Convex(C^5) = \text{FALSE}$, $C^6(z^3, z^4)$, with $Is_Convex(C^5) = \text{TRUE}$, and $C^7(z^3, z^4)$, with $Is_Convex(C^5) = \text{FALSE}$, such that all points in each subspace satisfy Equation (7) or (8).

The overall results are shown in Tables 4, and Figures 12-15. Note that results with the SD algorithm are not presented in Table 4 nor in Figure 13 for problem TNK, since there are no convex parts on the Pareto front and solutions other than the anchor points cannot be identified, as can be seen in Figure 12(a).

From the tabulated and graphical results, we can conclude that the SDNBI algorithm outperforms the SD algorithm and the mNBI method in all metrics except for $t_{cpu,t}$ and $t_{cpu,a}$. The higher total computational cost of SDNBI may be explained by the additional calculation procedures for: the generation of inner and outer approximations of the Pareto front; the removal of subspaces that do not contain Pareto points, and the addition of objective constraints inherent in the mNBI subproblem. At the 20th iteration, the SDNBI algorithm identifies all disconnected regions of the Pareto front, with confidence that no Pareto points exist in these areas. By solving the (mNBI $\bar{n}(a)$) subproblems, not only two empty regions are discarded, but new Pareto points are identified. As a result, the SDNBI algorithm succeeds in improving the Pareto approximation efficiently at each

iteration, whilst the performance of the mNBI is limited when it encounters a large disconnected region. These aspects are illustrated in Figures 13 and 15, where the progress of each quality measure can be compared. As can be seen in Figure 13(d) the differences in $t_{cpu,a}$ between the algorithms decreases despite the rapid increase in $t_{cpu,t}$ with SDNBI (see Figure 13(e)), since a larger number of Pareto points (N_{unq}) are identified with SDNBI as iterations proceed. In Figure 15(d), lower values of $t_{cpu,a}$ are observed with SDNBI after the 25th iteration compared to mNBI, as a result of identifying more Pareto points. This suggests that the SDNBI algorithm may be more computationally efficient when the Pareto front consists of many disconnected regions.

6.4. Test problem ZDT5

The results for test problem ZDT5 obtained with SD, mNBI and SDNBI for 40 iterations are summarized in Table 4 and Figures 16 and 17. For this test problem, the true Pareto front is represented as a set of 31 integer Pareto points and the SDNBI identifies the complete set of solutions for a given tolerance, while the mNBI method and the SD algorithm appear to be relatively ineffective in achieving high performance in DM and N_{unq} with the given number of iterations. These results demonstrate the effectiveness of the SDNBI algorithm at finding a diverse and accurate set of Pareto points over the discrete bi-objective domain. As can be observed in Figure 17(d), the performance of the SDNBI algorithm in terms of $t_{cpu,a}$ improves as iterations proceed with the lowest computational cost is obtained at iteration 40, by which convergence is reached.

In order to investigate how the SDNBI algorithm works when the complete Pareto set has been identified, the convergence tolerance ϵ is reduced to 10^{-3} and all algorithms are run for the number of iterations required to reach this tolerance with SDNBI. As can be seen in Figure 17(d), the $t_{cpu,a}$ values increase rapidly with the SDNBI algorithm as no new Pareto points can be found following the identification of the complete set of Pareto points (at 40th iteration). This additional cost is associated with the solution of the subproblems (mNBI $\bar{n}(a)$) and (mNBI $\bar{n}(b)$) through which facets are removed, but no additional Pareto points are identified. It is notable that all regions where no Pareto point exists are removed from the search space after 61 iterations (see Figure 17). This allows the SDNBI algorithm to terminate although the pre-defined error tolerance, ϵ , is not satisfied. Although not shown here, without setting a maximum number of iterations, the SD algorithm would iterate until there are no remaining facets to be investigated (at the 66th iteration).

As can be observed from Figure 17(c), by iteration 56, all 31 Pareto points have been identified with the mNBI method. However, β values could be enumerated until the 87th iteration, when the set of possible choices

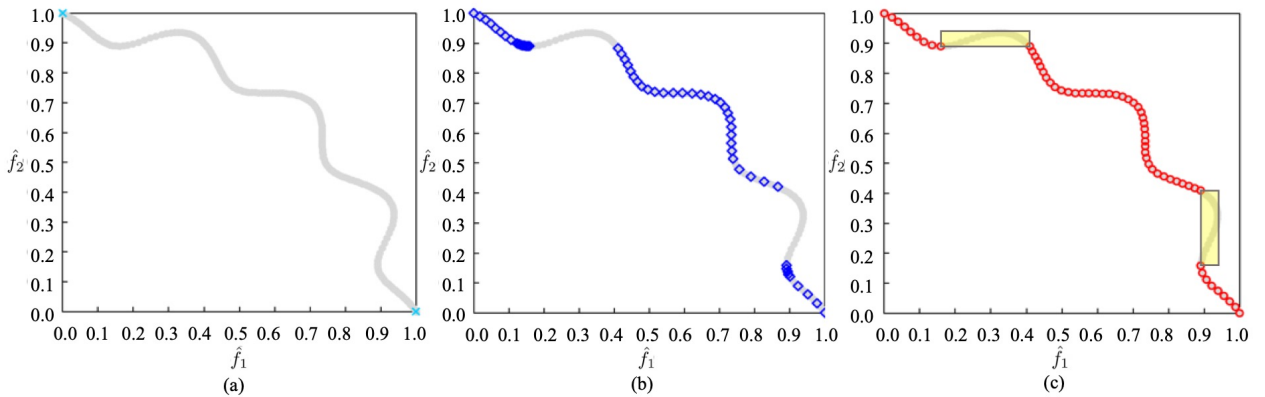


Figure 12: Pareto points generated by (a) the SD algorithm (\times), (b) the mNBI method (\triangle), and (c) the SDNBI algorithm (\circ) for test problem TNK, including the regions discarded as being devoid of Pareto points (yellow shading). The best-known Pareto front is shown in grey.

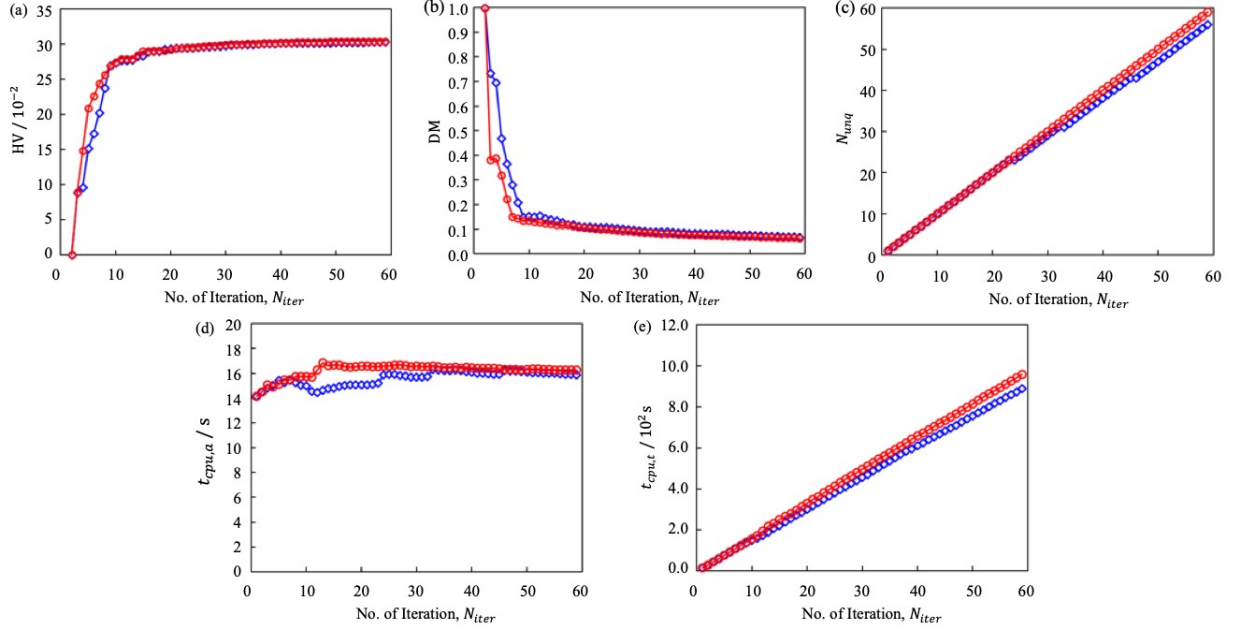


Figure 13: Performance metrics as a function of iteration number for the application of the mNBI ($\text{--}\diamond\text{--}$) and SDNBI ($\text{--}\circ\text{--}$) algorithms to problem TNK for 59 iterations: (a) Scaled hypervolume, HV, (b) Scaled distribution metric, DM, (c) Number of unique Pareto points, N_{unq} , (d) CPU time spent per iteration in seconds, $t_{cpu,a}$, (e) overall CPU time in seconds, $t_{cpu,t}$.

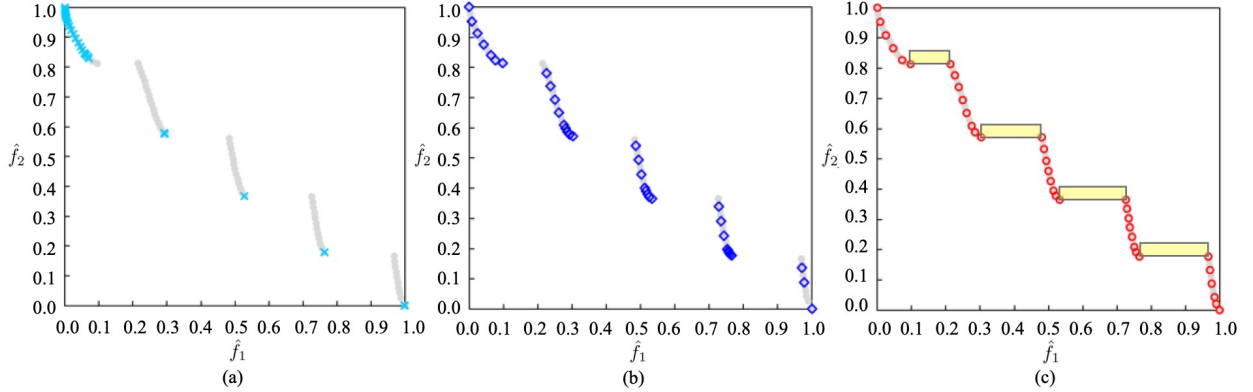


Figure 14: Pareto points generated by (a) SD algorithm (\times), (b) mNBI (\triangle), and (c) SDNBI (\circ) for the test problem ZDT3, including the regions discarded as being devoid of Pareto points (yellow shading). The best-known Pareto front is shown in grey.

of reference points, $\Phi\beta$, becomes almost empty. This suggests that the mNBI method can fail to recognize that all Pareto points have been found when a highly disconnected or discrete Pareto front is involved, due to the use of an arbitrary termination criterion.

7. Conclusions

A novel algorithm, SDNBI, that combines features of the SD and NBI methods with the aim of generating accurate approximations of nonconvex and combinatorial Pareto fronts in bi-objective space has been presented. The main benefits of the proposed algorithm are focused on the exploration of nonconvex regions of the Pareto front and on the identification of regions where no further nondominated solution exists, indicating that parts of the Pareto front are disconnected. Key aspects of the SDNBI algorithm include: 1) the characterization of inner and outer approximations such that the accuracy of the incumbent set of Pareto points can be assessed during the course of the algorithm, 2) a systematic way of setting the scalarization parameters of the mNBI

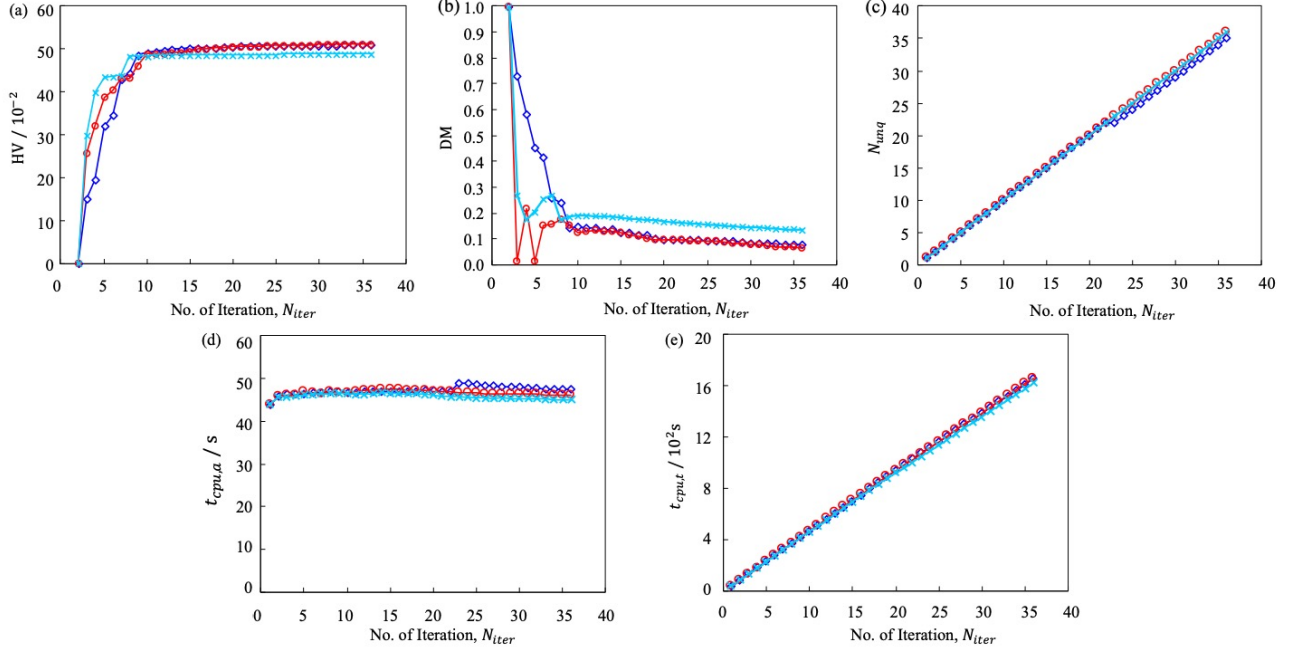


Figure 15: Performance metrics as a function of iteration number for the application of the SD algorithm (\times), mNBI method (\diamond), and SDNBI algorithm (\circ) to ZDT3 for 36 iterations: (a) Scaled hypervolume, HV, (b) Scaled distribution metric, DM, (c) Number of unique Pareto points, N_{unq} , (d) CPU time spent per iteration in seconds, $t_{cpu,a}$, (e) overall CPU time in seconds, $t_{cpu,t}$.

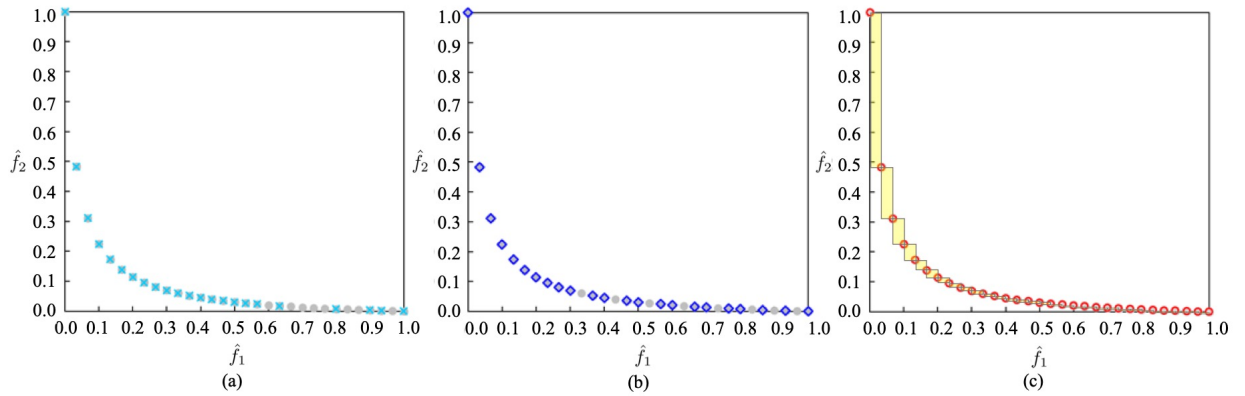


Figure 16: Pareto points (z) generated by the (a) SD algorithm (\times), (b) the mNBI method (\triangle), and (c) the SDNBI algorithm (\circ) for test problem ZDT5 with $N_{iter,fix} = 40$, including the regions discarded as being devoid of Pareto points (yellow shading). The grey points represent the set all Pareto points.

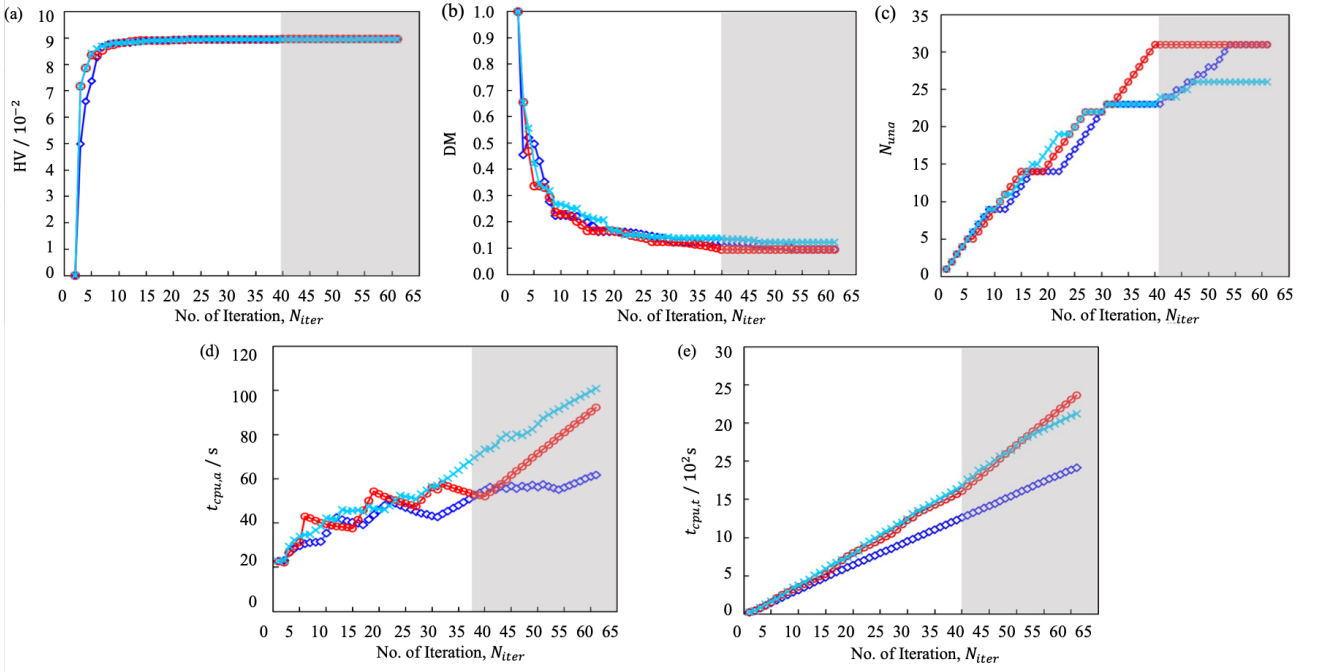


Figure 17: Performance metrics as a function of iteration number for the application of the SD ($- \times -$), mNBI ($- \diamond -$), and SDNBI algorithms ($- \circ -$) to ZDT5 for up to 64 iterations. The white area corresponds to the 40 iterations consistent with the SDNBI stopping criterion, while the grey shaded area corresponds to additional iterations needed for eliminating all empty area and so terminating the algorithm before reaching the stopping tolerance.

subproblem, 3) the decomposition of an objective space based on the convexity and nonconvexity of parts of the Pareto front, and 4) the refinement of the scalarized subproblem to avoid unnecessary iterations over disconnected or empty regions of the objective space.

To assess the performance of the proposed algorithm, numerical tests were conducted for five bi-objective benchmark problems (MOP1, SCH2, TNK, ZDT3, and ZDT5). The performance of the algorithm in terms of the accuracy of the approximation of the Pareto front constructed in disconnected nonconvex objective domains were compared to two MOO approaches: the SD algorithm and the mNBI method. This provided clear evidence of the effectiveness of the SDNBI algorithm in generating a more diverse and better-distributed set of Pareto points over disconnected and/or nonconvex Pareto fronts compared to the approximations generated with the mNBI method and the SD algorithm. The solution of test problem ZDT5, in which the true Pareto front comprises 31 discrete points, highlighted the robustness of the SDNBI algorithm: the complete set of Pareto points was generated with relatively few iterations, leading to high computational efficiency. The SDNBI not only provides information on the quality of the Pareto front approximation (as does the SD algorithm), but it also reveals areas of bi-objective space that are devoid of Pareto point.

Further work will focus on testing the SDNBI algorithm on additional literature and engineering problems to derive general conclusions on the performance of physical problems. Extending the approach to handle problems with three or more objective functions will also be considered in future work.

Acknowledgements

Ye Seol Lee gratefully acknowledges financial support from the Fund For Women Graduates (FfWG) of the British Federation of Women Graduates and from Imperial College London via a Roger Sargent scholarship.

Data Availability

Code for the SD algorithm, mNBI method, and SDNBI is available at <https://github.com/MolChemML/MOO-SDNBI>, and all data pertaining to the results are available on the Zenodo repository (<https://doi.org/10.5281/zenodo.11223677>), under CC-BY licence.

References

- Andersson, T., Nowak, D., Johnson, T., Mark, A., Edelvik, F., & Küfer, K.-H. (2018). Multiobjective optimization of a heat-sink design using the sandwiching algorithm and an immersed boundary conjugate heat transfer solver. *Journal of Heat Transfer*, *140*. doi:[10.1115/1.4040086](https://doi.org/10.1115/1.4040086).
- Belotti, P., Soylu, B., & Wiecek, M. M. (2013). A branch-and-bound algorithm for biobjective mixed-integer programs. *Optimization Online*, .
- Benson, H. P. (1998). An outer approximation algorithm for generating all efficient extreme points in the outcome set of a multiple objective linear programming problem. *Journal of Global Optimization*, *13*, 1–24. doi:[10.1023/A:1008215702611](https://doi.org/10.1023/A:1008215702611).
- Benson, H. P., & Sayin, S. (1997). Towards finding global representations of the efficient set in multiple objective mathematical programming. *Naval Research Logistics (NRL)*, *44*, 47–67.
- Bokrantz, R., & Forsgren, A. (2013). An algorithm for approximating convex pareto surfaces based on dual techniques. *INFORMS Journal on Computing*, *25*, 377–393. doi:[10.1287/ijoc.1120.0508](https://doi.org/10.1287/ijoc.1120.0508).
- Bortz, M., Burger, J., Asprion, N., Blagov, S., Böttcher, R., Nowak, U., Scheithauer, A., Welke, R., Küfer, K.-H., & Hasse, H. (2014). Multi-criteria optimization in chemical process design and decision support by navigation on pareto sets. *Computers & chemical engineering*, *60*, 354–363. doi:[10.1016/j.compchemeng.2013.09.015](https://doi.org/10.1016/j.compchemeng.2013.09.015).
- Burger, J., Papaioannou, V., Gopinath, S., Jackson, G., Galindo, A., & Adjiman, C. S. (2015). A hierarchical method to integrated solvent and process design of physical CO₂ absorption using the SAFT- γ Mie approach. *AIChE Journal*, *61*, 3249–3269. doi:[10.1002/aic.14838](https://doi.org/10.1002/aic.14838).
- Craft, D. L., Halabi, T. F., Shih, H. A., & Bortfeld, T. R. (2006). Approximating convex pareto surfaces in multiobjective radiotherapy planning. *Medical physics*, *33*, 3399–3407. doi:[10.1118/1.2335486](https://doi.org/10.1118/1.2335486).
- Das, I., & Dennis, J. E. (1998). Normal-boundary intersection: A new method for generating the pareto surface in nonlinear multicriteria optimization problems. *SIAM Journal on Optimization*, *8*, 631–657. doi:[10.1137/S1052623496307510](https://doi.org/10.1137/S1052623496307510).
- Deb, K. (2001). *Multi-objective optimization using evolutionary algorithms* volume 16. John Wiley & Sons.
- Deb, K., Agrawal, S., Pratap, A., & Meyarivan, T. (2000). A fast elitist non-dominated sorting genetic algorithm for multi-objective optimization: NSGA-II. In *International conference on parallel problem solving from nature* (pp. 849–858). Springer.
- Deb, K., & Jain, H. (2013). An evolutionary many-objective optimization algorithm using reference-point-based nondominated sorting approach, part I: solving problems with box constraints. *IEEE transactions on evolutionary computation*, *18*, 577–601. doi:[10.1109/TEVC.2013.2281535](https://doi.org/10.1109/TEVC.2013.2281535).
- Drud, A. S. (1994). CONOPT—a large-scale grg code. *ORSA Journal on computing*, *6*, 207–216.

- Ehrgott, M. (2005a). *Multicriteria optimization* volume 491. Springer Science & Business Media.
- Ehrgott, M. (2005b). *Multicriteria Optimization, Lecture Notes in Economics and Mathematical Systems* volume 491. Springer.
- Ehrgott, M., Shao, L., & Schöbel, A. (2011). An approximation algorithm for convex multi-objective programming problems. *Journal of Global Optimization*, 50, 397–416. doi:[10.1007/s10898-010-9588-7](https://doi.org/10.1007/s10898-010-9588-7).
- Gill, P. E., Murray, W., & Saunders, M. A. (2005). SNOPT: An SQP algorithm for large-scale constrained optimization. *SIAM review*, 47, 99–131.
- Graham, E. J., Forte, E., Burger, J., Galindo, A., Jackson, G., & Adjiman, C. S. (2022). Multi-objective optimization of equation of state molecular parameters: SAFT-VR Mie models for water. *Computers & Chemical Engineering*, 167, 108015. doi:[10.1016/j.compchemeng.2022.108015](https://doi.org/10.1016/j.compchemeng.2022.108015).
- Grossmann, I. E., Viswanathan, J., Vecchietti, A., Raman, R., Kalvelagen, E. et al. (2002). GAMS/DICOPT: A discrete continuous optimization package. *GAMS Corporation Inc*, 37, 55.
- Huang, H.-Z., Gu, Y.-K., & Du, X. (2006). An interactive fuzzy multi-objective optimization method for engineering design. *Engineering Applications of Artificial Intelligence*, 19, 451–460. doi:[10.1016/j.engappai.2005.12.001](https://doi.org/10.1016/j.engappai.2005.12.001).
- Ismail-Yahaya, A., & Messac, A. (2002). Effective generation of the pareto frontier using the normal constraint method. In *40th AIAA Aerospace Sciences Meeting & Exhibit* (p. 178). doi:[10.2514/6.2002-178](https://doi.org/10.2514/6.2002-178).
- Kim, I. Y., & De Weck, O. L. (2005). Adaptive weighted-sum method for bi-objective optimization: Pareto front generation. *Structural and multidisciplinary optimization*, 29, 149–158. doi:[10.1007/s00158-004-0465-1](https://doi.org/10.1007/s00158-004-0465-1).
- Klamroth, K., Tind, J., & Wiecek, M. M. (2003). Unbiased approximation in multicriteria optimization. *Mathematical Methods of Operations Research*, 56, 413–437. doi:[10.1007/s001860200217](https://doi.org/10.1007/s001860200217).
- Lee, Y. S., Graham, E. J., Galindo, A., Jackson, G., & Adjiman, C. S. (2020). A comparative study of multi-objective optimization methodologies for molecular and process design. *Computers & Chemical Engineering*, 136, 106802. doi:[10.1016/j.compchemeng.2020.106802](https://doi.org/10.1016/j.compchemeng.2020.106802).
- Li, H., Deb, K., Zhang, Q., Suganthan, P. N., & Chen, L. (2019). Comparison between MOEA/D and NSGA-III on a set of novel many and multi-objective benchmark problems with challenging difficulties. *Swarm and Evolutionary Computation*, 46, 104–117. doi:[10.1016/j.swevo.2019.02.003](https://doi.org/10.1016/j.swevo.2019.02.003).
- Lim, Y. I., Floquet, P., & Joulia, X. (2001). Efficient implementation of the normal boundary intersection (nbi) method on multiobjective optimization problems. *Industrial & engineering chemistry research*, 40, 648–655. doi:[10.1021/ie000400v](https://doi.org/10.1021/ie000400v).
- Logist, F., Houska, B., Diehl, M., & Van Impe, J. (2010). Fast pareto set generation for nonlinear optimal control problems with multiple objectives. *Structural and Multidisciplinary Optimization*, 42, 591–603. doi:[10.1007/s00158-010-0506-x](https://doi.org/10.1007/s00158-010-0506-x).
- Luenberger, D. G. (1997). *Optimization by vector space methods*. John Wiley & Sons.
- Marler, R. T., & Arora, J. S. (2004). Survey of multi-objective optimization methods for engineering. *Structural and multidisciplinary optimization*, 26, 369–395. doi:[10.1007/s00158-003-0368-6](https://doi.org/10.1007/s00158-003-0368-6).

- Messac, A., Ismail-Yahaya, A., & Mattson, C. A. (2003). The normalized normal constraint method for generating the pareto frontier. *Structural and multidisciplinary optimization*, 25, 86–98. doi:[10.1007/s00158-002-0276-1](#).
- Messac, A., & Mattson, C. A. (2004). Normal constraint method with guarantee of even representation of complete pareto frontier. *AIAA journal*, 42, 2101–2111. doi:[10.2514/1.8977](#).
- Miettinen, K. (1998). *Nonlinear Multiobjective Optimization* volume 12. Springer.
- Murray, W. (1997). Sequential quadratic programming methods for large-scale problems. *Computational Optimization and Applications*, 7, 127–142.
- Pál, L. (2013). Comparison of multistart global optimization algorithms on the BBOB noiseless testbed. In *Proceedings of the 15th annual conference companion on Genetic and evolutionary computation* (pp. 1153–1160). ACM. doi:[10.1145/2464576.2482693](#).
- Przybylski, A., & Gandibleux, X. (2017). Multi-objective branch and bound. *European Journal of Operational Research*, 260, 856–872. doi:[10.1016/j.ejor.2017.01.032](#).
- Rennen, G., Van Dam, E. R., & Den Hertog, D. (2011). Enhancement of sandwich algorithms for approximating higher-dimensional convex pareto sets. *INFORMS Journal on Computing*, 23, 493–517. doi:[10.1287/ijoc.1100.0419](#).
- Schaffer, J. D. (1984). *Multiple objective optimization with vector evaluated genetic algorithms*. Ph.D. thesis Vanderbilt University.
- Schott, J. R. (1995). *Fault tolerant design using single and multicriteria genetic algorithm optimization*. Ph.D. thesis Massachusetts Institute of Technology.
- Serafini, P. (1994). Simulated annealing for multi objective optimization problems. In *Multiple criteria decision making* (pp. 283–292). Springer.
- Shao, L., & Ehrgott, M. (2007). Finding representative nondominated points in multiobjective linear programming. In *2007 IEEE Symposium on Computational Intelligence in Multi-Criteria Decision-Making* (pp. 245–252). IEEE. doi:[10.1109/MCDM.2007.369446](#).
- Shao, L., & Ehrgott, M. (2008). Approximating the nondominated set of an molp by approximately solving its dual problem. *Mathematical Methods of Operations Research*, 68, 469–492. doi:[10.1007/s00186-008-0220-2](#).
- Shao, L., & Ehrgott, M. (2016). Discrete representation of non-dominated sets in multi-objective linear programming. *European Journal of Operational Research*, 255, 687–698. doi:[10.1016/j.ejor.2016.05.001](#).
- Shukla, P. K. (2007). On the normal boundary intersection method for generation of efficient front. In *International Conference on Computational Science* (pp. 310–317). Springer.
- Siddiqui, S., Azarm, S., & Gabriel, S. A. (2012). On improving normal boundary intersection method for generation of pareto frontier. *Structural and Multidisciplinary Optimization*, 46, 839–852. doi:[10.1007/s00158-012-0797-1](#).

- Simab, M., Javadi, M. S., & Nezhad, A. E. (2018). Multi-objective programming of pumped-hydro-thermal scheduling problem using normal boundary intersection and vikor. *Energy*, *143*, 854–866. doi:[10.1016/j.energy.2017.09.144](https://doi.org/10.1016/j.energy.2017.09.144).
- Sobol', I. M., Asotsky, D., Kreinin, A., & Kucherenko, S. (2011). Construction and Comparison of High-Dimensional Sobol' Generators. *Wilmott*, *2011*, 64–79. doi:[10.1002/wilm.10056](https://doi.org/10.1002/wilm.10056).
- Solanki, R. S., Appino, P. A., & Cohon, J. L. (1993). Approximating the noninferior set in multiobjective linear programming problems. *European Journal of Operational Research*, *68*, 356–373. doi:[10.1016/0377-2217\(93\)90192-P](https://doi.org/10.1016/0377-2217(93)90192-P).
- Tanaka, M., Watanabe, H., Furukawa, Y., & Tanino, T. (1995). Ga-based decision support system for multi-criteria optimization. In *1995 IEEE International Conference on Systems, Man and Cybernetics. Intelligent Systems for the 21st Century* (pp. 1556–1561). IEEE volume 2.
- Vahidinasab, V., & Jadid, S. (2010). Normal boundary intersection method for suppliers' strategic bidding in electricity markets: An environmental/economic approach. *Energy Conversion and Management*, *51*, 1111–1119. doi:[10.1016/j.enconman.2009.12.019](https://doi.org/10.1016/j.enconman.2009.12.019).
- Van Veldhuizen, D. A., & Lamont, G. B. (1999). Multiobjective evolutionary algorithm test suites. In *Proceedings of the 1999 ACM symposium on Applied computing* (pp. 351–357).
- Wu, J., & Azarm, S. (2001). Metrics for quality assessment of a multiobjective design optimization solution set. *J. Mech. Des.*, *123*, 18–25. doi:[10.1115/1.1329875](https://doi.org/10.1115/1.1329875).
- Zheng, K., Yang, R.-J., Xu, H., & Hu, J. (2017). A new distribution metric for comparing pareto optimal solutions. *Structural and multidisciplinary Optimization*, *55*, 53–62. doi:[10.1007/s00158-016-1469-3](https://doi.org/10.1007/s00158-016-1469-3).
- Zimmermann, H.-J. (1978). Fuzzy programming and linear programming with several objective functions. *Fuzzy sets and systems*, *1*, 45–55. doi:[10.1016/0165-0114\(78\)90031-3](https://doi.org/10.1016/0165-0114(78)90031-3).
- Zitzler, E., Deb, K., & Thiele, L. (2000). Comparison of multiobjective evolutionary algorithms: Empirical results. *Evolutionary Computation*, *8*, 173–195. doi:[10.1162/106365600568202](https://doi.org/10.1162/106365600568202).
- Zitzler, E., Thiele, L., Laumanns, M., Fonseca, C. M., & Da Fonseca, V. G. (2003). Performance assessment of multiobjective optimizers: An analysis and review. *IEEE Transactions on Evolutionary Computation*, *7*, 117–132. doi:[10.1109/TEVC.2003.810758](https://doi.org/10.1109/TEVC.2003.810758).